NATIONAL BUREAU OF STANDARDS REPORT

4037

SHRINKAGE STRESSES IN MASONRY WALLS

PROGRESS REPORT NO. 2

by

Sven D. Svendsen, D. Watstein and S. Levy

<NBS>

U. S. DEPARTMENT OF COMMERCE
NATIONAL BUREAU OF STANDARDS

THE NATIONAL BUREAU OF STANDARDS

The scope of activities of the National Bureau of Standards is suggested in the following listing of the divisions and sections engaged in technical work. In general, each section is engaged in specialized research, development, and engineering in the field indicated by its title. A brief description of the activities, and of the resultant reports and publications, appears on the inside of the back cover of this report.

Electricity and Electronics. Resistance and Reactance. Electron Tubes. Electrical Instruments. Magnetic Measurements. Process Technology. Engineering Electronics. Electronic Instrumentation. Electrochemistry.

Optics and Metrology. Photometry and Colorimetry. Optical Instruments. Photographic Technology. Length. Engineering Metrology.

Heat and Power. Temperature Measurements. Thermodynamics. Cryogenic Physics. Engines and Lubrication. Engine Fuels.

Atomic and Radiation Physics. Spectroscopy. Radiometry. Mass Spectrometry. Solid State Physics. Electron Physics. Atomic Physics. Nuclear Physics. Radioactivity. X-rays. Betatron. Nucleonic Instrumentation. Radiological Equipment. AEC Radiation Instruments.

Chemistry. Organic Coatings. Surface Chemistry. Organic Chemistry. Analytical Chemistry. Inorganic Chemistry. Electrodeposition. Gas Chemistry. Physical Chemistry. Thermochemistry. Spectrochemistry. Pure Substances.

Mechanics. Sound. Mechanical Instruments. Fluid Mechanics. Engineering Mechanics. Mass and Scale. Capacity, Density, and Fluid Meters. Combustion Controls.

Organic and Fibrous Materials. Rubber. Textiles. Paper. Leather. Testing and Specifications. Polymer Structure. Organic Plastics. Dental Research.

Metallurgy. Thermal Metallurgy. Chemical Metallurgy. Mechanical Metallurgy. Corrosion.

Mineral Products. Porcelain and Pottery. Glass. Refractories. Enameled Metals. Concreting Materials. Constitution and Microstructure.

Building Technology. Structural Engineering. Fire Protection. Heating and Air Conditioning. Floor, Roof, and Wall Coverings. Codes and Specifications.

Applied Mathematics. Numerical Analysis. Computation. Statistical Engineering. Mathematical Physics.

Data Processing Systems. Components and Techniques. Digital Circuitry. Digital Systems. Analogue Systems.

Cryogenic Engineering. Cryogenic Equipment. Cryogenic Processes. Properties of Materials. Gas Liquefaction.

Radio Propagation Physics. Upper Atmosphere Research. Ionospheric Research. Regular Propagation Services.

Radio Propagation Engineering. Frequency Utilization Research. Tropospheric Propagation Research.

Radio Standards. High Frequency Standards. Microwave Standards.

● Office of Basic Instrumentation　　　　　　　　● Office of Weights and Measures

NATIONAL BUREAU OF STANDARDS REPORT

SHRINKAGE STRESSES IN MASONRY WALLS

PROGRESS REPORT NO. 2

by

Sven D. Svendsen, D. Watstein and S. Levy

To
Office of the Chief of Engineers
Department of the Army

Bureau of Yards and Docks
Department of the Navy
and

Assistant Chief of Staff
Department of the Air Force

⟨NBS⟩

U. S. DEPARTMENT OF COMMERCE
NATIONAL BUREAU OF STANDARDS

SHRINKAGE STRESSES IN MASONRY WALLS
PROGRESS REPORT NO. 2

by

Svend D. Svendsen, D. Watstein and S. Levy

Abstract

The current progress report presents the development
of the elastic theory for stresses in a wall which
undergoes shrinkage while its lower edge is restrained
from shrinking by a rigid footing. The solution ob-
tained is represented by an infinite set of equations.
In the numerical solutions presented, the finite number
of equations and coefficients selected in each case was
such as to give adequate agreement between the given
boundary conditions and the computed boundary stresses
and displacements.

The numerical solutions were obtained for a wall having
a length of twice its height. Work is in progress for
walls in which the length and height are equal and in
which the length is four times the height. These solu-
tions are based on the assumption that the footing is
sufficiently rigid to prevent all shortening along the
attachment line. A numerical solution is also being ob-
tained for a wall having a length of twice its height,
with non-uniform footing restraint.

The theoretical results are being checked by noting
stresses in plaster and concrete models. The work thus
far has been confined to walls having a length of twice
the height, with two different degrees of restraint pro-
vided by footings of different sizes. The agreement be-
tween the theoretical and observed values of principal
stress at several selected points was fair. It was noted
that the agreement between the observed and computed
stresses improved for points further removed from the free
edge of the wall.

Further experimental work is being planned with models of
concrete containing internal strain gages to determine
strains in walls undergoing actual shrinkage.

---

1. INTRODUCTION

A newly constructed masonry wall contains as a rule a considerable amount of moisture. As the wall dries out, it undergoes shrinkage whose magnitude depends on the type of construction and the properties of the materials used. A similar tendency to shorten is caused by thermal contraction when the temperature on one or both sides of the wall decreases.

In most cases, however, the wall is only a part of a larger structure and hence is not free to contract. It is normally restrained by other parts of the construction, for instance by adjoining walls and floors, and especially by its own foundation. The foundation, which can be a basement wall or a footing, is usually more rigid and has less tendency to contract than the wall itself. The restraint, the magnitude of which primarily depends on the rigidity of the structural parts involved, causes stresses in the wall which eventually may result in cracks.

The investigation described in this report is the first part of a study of the distribution and intensity of shrinkage stresses in contracting masonry walls restrained from shortening at the foundation level. The study falls in two parts:

(a) An experimental investigation of the stresses carried out with wall models by the Structural Engineering Section.

(b) A theoretical analysis of the problem and development of mathematical expressions for the stresses in the walls. This analysis is being carried out by the Engineering Mechanics Section.

The first steps of the study are described in Progress Report No. 1, dated June 18, 1954.

2. EXPERIMENTAL TESTS WITH WALL MODELS

The shortening of walls due to shrinkage and thermal contraction was assumed to be an entirely elastic deformation in this study. As the models for practical reasons have to be made considerably smaller than the prototypes (a scale of about 1/5 is used), it was necessary to employ materials with a high degree of homogeneity and elasticity for the models.

In order to simplify the tests, they were confined to those concerned with shrinkage and thermal contraction alone. No vertical loads which would represent the loads from floors, roof and walls were applied. It was assumed that the effect of such loads can be estimated and the resultant stresses computed through the principle of superposition.

It was further assumed that the foundation is very rigid in comparison with the wall and that the bond between them is sufficiently strong to prevent displacement of the wall relative to the foundation.

2.1 Materials and description of models

The first models described in Progress Report No. 1 were made of a special rubber having a modulus of elasticity of about 650 psi and a Poisson's ratio of 0.5. The tests with these models, however, did not give satisfactory results and the rubber was accordingly replaced with plaster of Paris and concrete in all subsequent work.

The plaster of Paris used was a high strength gypsum known as Hydrocal. The proportions of the mix used in the models reported herein, were 2.5 parts of plaster to 1 part of water, by weight, and the compressive strength was about 4000 psi. This mix had a modulus of elasticity of 2.15×10^6 psi and a Poisson's ratio of 0.28, as determined with sonic resonance tests on 2- by 4-in. cylinders. Some preliminary tests were made with other mixes ranging in proportions from 2.25-3.0 parts of plaster to 1 part of water. The values of Young's modulus determined for these mixes varied from 1.7×10^6 to 2.3×10^6 psi and Poisson's ratio from 0.17 to 0.28. In order to diminish the expansion of the plaster during the setting time, some mixes were made with various amounts of a special retarder added.

Two different mixes of concrete were used for models, both made with a high early strength portland cement. One of the mixes was proportioned, by weight, 1:2.5:2.0 with maximum size of gravel of 3/8 in.; the net water-cement ratio was 0.58 and the slump 4 in. Determined on three months old 6- by 12-in. cylinders, the compressive strength of this mix was 8160 psi, the modulus of elasticity 5.82×10^6 psi and Poisson's ratio 0.19. The corresponding values for the other mix were: proportions 1:3.1:2.6 w/c ratio 0.53, slump 1 1/4 in., compressive strength 5800 psi, modulus of elasticity 5.67×10^6 and Poisson's ratio 0.16. This mix also

contained Vinsol Resin in the amount of 0.006 percent by weight of cement.

The form and size of the concrete and plaster models are shown in figure 1. To prevent curvature of the line where the wall is attached to the foundation strip during the test, the specimen was made symmetrical with a wall attached to each side of the foundation strip. The size of the walls was the same for all models, the length being twice the height, but the foundation strip was made with two different cross sections, 3 1/2 in. by 4 1/4 in. and 6 1/4 in. by 4 1/4 in. The rubber models had the same form, but they were smaller, with 18- by 9- by 1-in. walls and a 2- by 4- by 22-in. foundation strip.

2.2. Test methods

It can be readily appreciated that a test procedure for determining stresses in masonry walls caused by actual drying shrinkage poses a number of experimental difficulties and takes a long time to carry out. For this reason, the experimental work in this study was confined to models in which shrinkage stresses were simulated by a suitable loading procedure. The analogy between the two testing methods is shown in figure 2. If the wall is placed on a footing which imposes no restraint (2a), the free shrinkage will cause a contraction which in an exaggerated manner, is indicated by the dotted lines. A very rigid foundation, representing 100 percent restraint, will correspondingly cause the wall to deform in a manner similar to that in 2b. If the foundation of the wall 2a, which was permitted to shrink freely, is now replaced with a rigid one, and this foundation is elongated by applying a tensile load, the result will be as shown in 2c. For a correctly chosen load, the longitudinal strains in walls 2b and 2c will be equal and the stresses in every point of the two walls will be the same.

In view of the relatively low extensibility of plaster and concrete, the models were actually loaded in compression instead of tension. A high compressive load was applied and the corresponding strains noted at various points were assumed to correspond to "zero stress" in the wall. Upon releasing the load until only a nominal load was imposed on the footing, the strains were again noted. Under the assumption that all deformation were within the elastic range, this procedure gave the same strains and stresses as a tensile load of the same magnitude as the difference between the initial and final compressive load.

The strains and stresses in walls and foundations were determined with bonded wire strain gages attached to the surface. Both single gages and 3 element rectangular rosettes were used, the latter giving the magnitude and direction of the principal stresses. Figure 3 shows one of the plaster models with some of the gages attached, placed in the testing machine.

The rubber models were tested with a tensile load applied to the ends of the foundation. The strains were determined by comparing the dimensions of a rectangular grid on the strained and unstrained wall. These tests did not give satisfactory results, partly because the modulus of elasticity of the rubber to a large extent varied with the stress history of the specimen. Another source of error was the fact that the grid did not provide markings which were precise enough or well enough defined. The fact that this test method gave no information about the shearing deformations, was also a serious disadvantage.

2.3. Wall with 3 1/2- by 4 1/4-in. foundation (type I)

Several models with a foundation of this size were made, all of them of plaster of Paris, but only one of the specimens was given a complete test. Figure 4 shows the distribution of bonded wire gages on this model, each station representing a gage on both front and back sides. Measurements were only made on one of the two walls, the several gages on the opposite wall being used only to check the symmetry of loading.

Figure 5 gives curves showing the distribution of the horizontal strain, averaged for both faces of the wall, in planes 1 to 6 (figure 4) for a load increment of 19,500 lb. Curves 1 and 2 show the deformations of the foundation at its centerline and at the top 3/4 in. from the face of the wall. The strains in these two planes agree surprisingly well but they show that the wall was only partially restrained by the foundation from shrinking. A restraint of 100 percent would have produced uniform strains along the entire length of the foundation, while in this case the strains near the center of the wall were only 45 percent of the strains at the free ends. The strains given in figure 5 show that the non uniform strain distribution, although quite marked, persisted only for a short distance from the corner. The strains 1 in. above the foundation, represented by curve 3 were almost uniform over most of the length. The large

difference between curve 3 and curves 1 and 2 near the ends
of the wall indicates, however, that the shear stresses in
these areas must be very high.

The magnitude of the strains decreased rapidly with the
height above the foundation, and the variation of the strain
near the ends became less abrupt. The top of the wall had
no contraction at all and a small expansion was recorded
near the centerline (curve 6).

Horizontal, vertical and principal stresses were com-
puted for points A to G (figure 4). The values given in
table 1 are these stresses divided by $E \times \epsilon_m$ where E is the
modulus of elasticity for the wall material and ϵ_m the strain
in the foundation at the center of the wall. The values are
in this way made independent of the properties of the material
and (to a certain degree) of the rigidity of the foundation.
All calculations are based on four different tests made over
a period of six months, and each point represents the average
of four different rosettes; α is the angle between the hori-
zontal axis and the principal tensile stress and $\alpha_{\prime}$ the
angle between the axis and the principal shear stress. Ten-
sile stresses were taken as positive, and compressive stresses
as negative.

The magnitude and direction of the principal tensile
and compressive stresses are also shown in figure 6. Even
though there are not enough data for a complete stress pic-
ture, the figure gives some interesting indications. The
principal tensile stresses are highest just above the founda-
tion, decreasing rapidly with the height near the edges and
somewhat slower near the center. The stresses are nearly
horizontal at the centerline and approach an upward direction
with the distance from this line. If the stresses become large
enough to cause cracks, they appear first at the bottom of the
wall at right angle to the direction of the principal tensile
stresses.

2.4. Wall with 6 1/4- by 4 1/4-in. foundation (type II)

Attempts were made to increase the restraint in the wall
by increasing the size of the foundation to 6 1/4- by 4 1/4 in.
Several models of this type were cast, both of plaster of Paris
and concrete with the size of the wall being the same as before.
This proved, however, to be a more difficult task than expected,
as most of these models developed cracks before testing or dur-
ing the loading of the specimen. The cracks occurred most

frequently at the bottom edge of the wall, but they also appeared in the foundation just below the wall.

In the plaster of Paris specimens the cracks were obviously due to the expansion of the material during the setting period while the strength was still very low. This expansion increased with the cross section and consequently was much larger for the foundation than for the wall. This caused a difference in strain along the boundary, and the wall had a tendency to crack at the bottom edge where it was sharply restrained from expansion by the mold. Attempts were made to diminish the expansion by using different amounts of a plaster retarder in the mix. This did not help, however, as the retarder only postponed the starting time of setting without decreasing the size of the deformation. Part of the expansion in plaster of Paris was thermal, and accordingly an attempt was made to cool the foundation with ice during its initial setting period. In this way it was possible to prevent cracks at the bottom edge of the wall, but the cooling seemed to increase the internal stresses and the tendency of cracking inside the foundation.

The cracks in the concrete models were probably due to a combination of thermal expansion during the first day's curing in the mold and the shrinkage of the specimen after it was taken out of the fog chamber. The thin wall dried out and shrank much faster than the foundation, and the shrinkage stresses in it developed in the same manner as in a restrained prototype. As shown in figure 6, these stresses may cause cracks which are almost horizontal at the bottom edge of the wall below and to the left of point A. In order to decrease the size of these stresses, models were made of a leaner mix with lower w/c ratio and given a longer curing time in the fog chamber. The results were somewhat better in that no visible cracks were observed, but the strain measurements were quite erratic and pointed to the existence of cracks in the interior of the models.

Figure 7 shows the foundation strains for a plaster model and a concrete model of this type. The irregularities of the curves, especially the difference in strain between the two ends of each foundation are probably due to internal cracks. In figure 8, the degrees of restraint of the two types of foundations are compared. The strain values are averaged for the left and right side, and they are given in percent of the

strain at the free ends. It will be seen that the restraint
at the centerline of the wall has increased from 46 percent
for the small foundation to 65 - 70 percent for the large.
The latter is probably still less than the restraint provided
by the foundation of actual masonry walls.

During the tests, some of the models were inadvertently
loaded to failure, with the rupture occurring in the wall.
The failure was due to cracks following one or both of two
different patterns. One type of cracking developed below
the wall and well within the foundation and was apparently
caused by tensile stresses both in the plane of the wall and
those forming a small angle with that plane. The other type
of crack followed an almost elliptical curve in the wall,
starting from the bottom corners. This type of crack can be
explained from the stress picture shown in figure 6. These
stresses are the result of a tensile load; a compressive
load would change the sign and thus give tensile stresses per-
pendicular to those caused by a tensile load. A crack due to
compression of the specimen will consequently have a tendency
to follow the direction of the stress arrows in figure 6.

Both of these crack patterns are evident on the nearest
wall of the model shown in figure 9.

2.5. Comparison of computed and observed stresses

Both the theoretical and the experimental part of the
study are far from complete and furnish, at the present time,
no basis for a valuation of results. In table 2, however,
the theoretical and experimental stress values are given for
the three locations A, E, and G, (see figure 6), on a model
with foundation 3 1/2- by 4 1/4 in. Figure 10 shows a com-
parison of the size and direction of the principal tensile
stress in these points. The theoretical values are computed
for a completely rigid foundation while the restraint during
the experimental tests was only 46 percent. Even so, the
stresses and directions seem to be in good agreement for E and
G. The location of A is very close to both the foundation and
the edge of the wall, and rather large discrepancies were to
be expected for this point.

2.6. Plans for future tests

As it seems to be very difficult to get a greater degree of restraint by casting the specimens integrally with a sufficiently rigid foundation, other methods will be tried in the future tests. A possible solution is indicated in figure 11. The double wall and the foundation strip is cast as a slab with uniform thickness and with bolt holes along the strip. When this slab is cured, the rigidness of the foundation will be increased by attaching a steel bar to each side of the strip and bolting slab and bars firmly together. Special care has to be taken to prevent any movement between slab and bars during the test.

By using this method, it should also be possible to determine stresses due to actual shrinkage. In this case internal strain gages will be used in the wall and the steel bars have to be attached while the slab is still saturated with moisture. The shrinkage stresses can then be determined by readings of the gages while the slab is drying. Walls with different ratio of height to length will be tested.

Several test specimens of the type described above were cast and tests are in progress.

3. ELASTIC THEORY FOR STRESS IN WALL RESTING ON A FOOTING

The construction of the wall is assumed to be such that, if it were unrestrained, it would shrink uniformly as it dries out. It is assumed that the footing restrains the shrinkage of the bottom of the wall. The equations will be derived in sufficiently general form to apply not only to the case of a footing sufficiently stiff to prevent all shortening and bending along the attachment line, but also to the case of a footing which is deformed by the shrinkage of the wall.

3.1. Equations for interior wall

The interior of the wall can be considered to be an elastic slab which obeys the customary equations of elasticity. We then have the equation,

$$\frac{\delta^4 \phi}{\delta x^4} + 2 \frac{\delta^4 \phi}{\delta x^2 \delta y^2} + \frac{\delta^4 \phi}{\delta y^4} = 0 \tag{1}$$

(See page 25, eq (26), of ref. 1)

The stress function ϕ in equation (1) is a function that, in a system of rectangular coordinates x and y in the plane of the wall, gives

$$\sigma_x = \delta^2\phi/\delta y^2 = \text{stress in x - direction}$$

$$\sigma_y = \delta^2\phi/\delta x^2 = \text{stress in y - direction}$$

$$\tau_{xy} = -\delta^2\phi/\delta x \, \delta y = \text{shear stress}$$

3.2. Boundary conditions

The boundary conditions at the top of the wall, $y = b$, figure 12, are

$$(\sigma_y)_{y=b} = 0; \quad (\tau_{xy})_{y=b} = 0 \qquad (2a)$$

An artificial boundary condition outside the wall along $y = o$ is included to obtain a convenient separation of even and odd terms in the final equations

$$(\sigma_y)_{y=o} = 0; \quad (\tau_{xy})_{y=o} = 0 \qquad (2b)$$

Along the sides $x = o$ and $x = a$, the boundary conditions are

$$(\sigma_x)_{x=o,a} = 0; \quad (\tau_{xy})_{x=o,a} = 0 \qquad (3)$$

Along the bottom of the wall, $y = b/2$, displacement boundary conditions apply. For a footing sufficiently stiff to prevent all shortening and bending, the conditions are

$$(\epsilon_x)_{y=b/2} = S/E \qquad (4)$$

and
$$(v)_{y=b/2} = 0 \qquad (5)$$

where S/E is the unit shortening _per unit of length_ due to shrinkage and E is Young's modulus. The vertical displacement is v.

3.3 Solution

No single expression satisfying equation (1) and the boundary conditions, equations (2) and (5), could be found. It was decided, therefore, to obtain a solution in the form of a series of expressions, each of which would identically satisfy equation (1) and the sum of which could be made to satisfy the boundary conditions (2) to (5) to any desired degree of accuracy. A comparison of the boundary values computed from the solution with the given values could then form a ready means of judging the adequacy of the solution.

Numerous expressions can be found to satisfy equation (1). In order to have a rapidly convergent solution, it is desirable that the expressions selected separate into groups, each of which primarily affects the stress along only one boundary. In each group it is desirable that the first term give a general picture of the stress, the first two give a somewhat finer picture, and so on.

The expressions selected for the solution apply every where in the plane except at x = 0, a, 2a,....and y = o, b/2, b, ... and can be written as

$$\phi = \sum_{m=1,3..} \sum_{n=1,2...} a_{m,n} \; \sin \frac{m\pi x}{a} \; \sin \frac{n\pi y}{b} \qquad (6a)$$

where,

$$\begin{array}{ll} a_{m,n} \\ (n, odd) \end{array} = \frac{n k_m + m t_n + (-1)^{\frac{n-1}{2}} p_m}{(m^2 \frac{b}{a} + n^2 \frac{a}{b})^2}$$

$$\begin{array}{ll} a_{m,n} \\ (n, even) \end{array} = \frac{n l_m + m t_n + (-1)^{\frac{n}{2}} n s_m}{(m^2 \frac{b}{a} + n^2 \frac{a}{b})^2}$$

12.

The k, ℓ, t, p, and s coefficients are determined by the bound-
ary conditions. An alternative form which is useful for deter-
mining stresses and displacements in the region o<x<a, b/2<y<b
is

$$\phi = \sum_{m=1,3\ldots} \frac{\pi^2 b}{16ma} K_m \left\{ \frac{\sinh\frac{m\pi y}{a}}{\cosh^2\frac{m\pi b}{2a}} + \frac{2y}{b} \frac{\sinh\frac{m\pi b}{2a}\left(1-\frac{2y}{b}\right)}{\cosh\frac{m\pi b}{2a}} \right\} \sin\frac{m\pi x}{a}$$

$$+ \sum_{m=1,3\ldots} \frac{\pi^2 b}{16ma} \ell_m \left\{ \frac{-\sinh\frac{m\pi y}{a}}{\sinh^2\frac{m\pi b}{2a}} + \frac{2y}{b} \frac{\cosh\frac{m\pi b}{2a}\left(1-\frac{2y}{b}\right)}{\sinh\frac{m\pi b}{2a}} \right\} \sin\frac{m\pi x}{a}$$

$$+ \sum_{n=1,2,3\ldots} \frac{\pi^2 a}{16 nb} t_n \left\{ \frac{\sinh\frac{n\pi x}{b}}{\cosh^2\frac{n\pi a}{2b}} + \frac{2x}{a} \frac{\sinh\frac{n\pi a}{2b}\left(1-\frac{2x}{a}\right)}{\cosh\frac{n\pi a}{2b}} \right\} \sin\frac{n\pi y}{b}$$

$$+ \sum_{m=1,3\ldots} \frac{\pi^2}{16 m^2} P_m \left\{ - \frac{\cosh\frac{m\pi b}{a}\left(\frac{y}{b}-\frac{1}{2}\right)}{\cosh^2\frac{m\pi b}{2a}} + \left(\frac{2y}{b}-1\right) \frac{\cosh\frac{m\pi b}{a}\left(1-\frac{y}{b}\right)}{\cosh\frac{m\pi b}{2a}} \right.$$

$$\left. + \frac{2a}{m\pi b} \frac{\sinh\frac{m\pi b}{a}\left(1-\frac{y}{b}\right)}{\cosh\frac{m\pi b}{2a}} \right\} \sin\frac{m\pi x}{a}$$

$$+ \sum_{m=1,3\ldots} \frac{\pi^2 b}{16ma} S_m \left\{ \frac{\left(\frac{y}{b}-\frac{1}{2}\right)\sinh\frac{m\pi b}{a}\left(\frac{3}{2}-\frac{y}{b}\right) - \left(\frac{3}{2}-\frac{y}{b}\right)\sinh\frac{m\pi b}{a}\left(\frac{y}{b}-\frac{1}{2}\right)}{\sinh^2\frac{m\pi b}{2a}} \right\}.$$

$$\sin\frac{m\pi x}{a}$$

(6b)

In equation (6a) and (6b) the summations involving the co-efficients k_m and ℓ_m primarily affect the stresses on the top of the wall, the summations involving the t_n coefficients primarily affect the stresses on the sides of the wall, and the summations involving the coefficients p_m and s_m primarily affect the stresses at the bottom of the wall.

The stress in the x direction is obtained from

$$\sigma_x = \frac{\delta^2 \phi}{\delta y^2} \tag{7}$$

as

$$\sigma_x = \sum_{m=1,3,\ldots} \frac{\pi^4 mb}{16a^3} k_m \sin \frac{m\pi x}{a} \left\{ \frac{\sinh \frac{m\pi y}{a}}{\cosh^2 \frac{m\pi b}{2a}} + \frac{2y}{b} \frac{\sinh \frac{m\pi b}{2a}\left(1-\frac{2y}{b}\right)}{\cosh \frac{m\pi b}{2a}} \right.$$

$$\left. - \frac{4a}{m\pi b} \frac{\cosh \frac{m\pi b}{2a}\left(1-\frac{2y}{b}\right)}{\cosh \frac{m\pi b}{2a}} \right\}$$

$$+ \sum_{m=1,3\ldots} \frac{\pi^4 mb}{16a^3} \ell_m \sin \frac{m\pi x}{a} \left\{ \frac{-\sinh \frac{m\pi y}{a}}{\sinh^2 \frac{m\pi b}{2a}} + \frac{2y}{b} \frac{\cosh \frac{m\pi b}{2a}\left(1-\frac{2y}{b}\right)}{\sinh \frac{m\pi b}{2a}} \right.$$

$$\left. - \frac{4a}{m\pi b} \frac{\sinh \frac{m\pi b}{2a}\left(1-\frac{2y}{b}\right)}{\sinh \frac{m\pi b}{2a}} \right\}$$

$$+ \sum_{n=1,2,3\ldots} \frac{\pi^4 na}{16b^3} t_n \sin \frac{n\pi y}{b} \left\{ \frac{-\sinh \frac{n\pi x}{b}}{\cosh^2 \frac{n\pi a}{2b}} - \frac{2x}{a} \frac{\sinh \frac{n\pi a}{2b}\left(1-\frac{2x}{a}\right)}{\cosh \frac{n\pi a}{2b}} \right\}$$

$$+ \sum_{m=1,3,\ldots} \frac{\pi^4}{16a^2} p_n \sin \frac{m\pi x}{a} \left\{ \frac{-\cosh \frac{m\pi b}{2a}\left(1-\frac{2y}{b}\right)}{\cosh^2 \frac{m\pi b}{2a}} + \left(\frac{2y}{b}-1\right)\frac{\cosh \frac{m\pi b}{a}\left(1-\frac{y}{b}\right)}{\cosh \frac{m\pi b}{2a}} - \frac{2a \sinh \frac{m\pi b}{a}\left(1-\frac{y}{b}\right)}{m\pi b \cosh \frac{m\pi b}{2a}} \right\}$$

$$+ \sum_{m=1,3\ldots} \frac{\pi^4 mb}{16a^3} s_n \frac{\sin \frac{m\pi x}{a}}{\sinh^2 \frac{m\pi b}{2a}} \left\{ \left(\frac{y}{b}-\frac{1}{2}\right)\sinh \frac{m\pi b}{a}\left(\frac{3}{2}-\frac{y}{b}\right) - \left(\frac{3}{2}-\frac{y}{b}\right)\sinh \frac{m\pi b}{a}\left(\frac{y}{b}-\frac{1}{2}\right) \right.$$

$$\left. - \frac{2a}{m\pi b}\cosh \frac{m\pi b}{a}\left(\frac{3}{2}-\frac{y}{b}\right) + \frac{2a}{m\pi b}\cosh \frac{m\pi b}{a}\left(\frac{y}{b}-\frac{1}{2}\right) \right\} \tag{8}$$

The stress in the y direction is similarly

$$\sigma_y = \sum_{m=1,3\ldots} \frac{\pi^4 mb}{16a^3} K_m \sin\frac{m\pi x}{a} \left\{ \frac{-\sinh\frac{m\pi y}{a}}{\cosh^2\frac{m\pi b}{2a}} - \frac{2y}{b} \frac{\sinh\frac{m\pi b}{2a}\left(1-\frac{2y}{b}\right)}{\cosh\frac{m\pi b}{2a}} \right\}$$

$$+ \sum_{m=1,3\ldots} \frac{\pi^4 mb}{16a^3} l_m \sin\frac{m\pi x}{a} \left\{ \frac{\sinh\frac{m\pi y}{a}}{\sinh^2\frac{m\pi b}{2a}} - \frac{2y}{b} \frac{\cosh\frac{m\pi b}{2a}\left(1-\frac{2y}{b}\right)}{\sinh\frac{m\pi b}{2a}} \right\}$$

$$+ \sum_{n=1,2,3,\ldots} \frac{\pi^4 na}{16b^3} t_n \sin\frac{n\pi y}{b} \left\{ \frac{\sinh\frac{n\pi x}{b}}{\cosh^2\frac{n\pi a}{2b}} + \frac{2x}{a} \frac{\sinh\frac{n\pi a}{2b}\left(1-\frac{2x}{a}\right)}{\cosh\frac{n\pi a}{2b}} \right.$$

$$\left. - \frac{4b}{n\pi a} \frac{\cosh\frac{n\pi a}{2b}\left(1-\frac{2x}{a}\right)}{\cosh\frac{n\pi a}{2b}} \right\}$$

$$+ \sum_{m=1,3\ldots} \frac{\pi^4}{16a^2} P_m \sin\frac{m\pi x}{a} \left\{ \frac{\cosh\frac{m\pi b}{2a}\left(1-\frac{2y}{b}\right)}{\cosh^2\frac{m\pi b}{2a}} - \left(\frac{2y}{b}-1\right) \frac{\cosh\frac{m\pi b}{a}\left(1-\frac{y}{b}\right)}{\cosh\frac{m\pi b}{2a}} \right.$$

$$\left. - \frac{2a}{m\pi b} \frac{\sinh\frac{m\pi b}{2a}\left(1-\frac{y}{b}\right)}{\cosh\frac{m\pi b}{2a}} \right\}$$

$$+ \sum_{m=1,3\ldots} \frac{\pi^4 mb}{16a^3} S_m \frac{\sin\frac{m\pi x}{a}}{\sinh^2\frac{m\pi b}{2a}} \left\{ -\left(\frac{y}{b}-\frac{1}{2}\right) \sinh\frac{m\pi b}{a}\left(\frac{3}{2}-\frac{y}{b}\right) \right.$$

$$\left. + \left(\frac{3}{2}-\frac{y}{b}\right) \sinh\frac{m\pi b}{a}\left(\frac{y}{b}-\frac{1}{2}\right) \right\}$$

$$(9)$$

The shearing stress is obtained from

$$\tau_{XY} = -\frac{\partial^2 \phi}{\partial x \partial y} \tag{10}$$

as

$$\tau_{XY} = \sum_{m=1,3...} \frac{\pi^4 mb}{16a^3} K_m \cos\frac{m\pi x}{a}\left\{ \frac{-\cosh\frac{m\pi y}{a}}{\cosh^2\frac{m\pi b}{2a}} + \frac{2y}{b}\,\frac{\cosh\frac{m\pi b}{2a}(1-\frac{2y}{b})}{\cosh\frac{m\pi b}{2a}} - \frac{2a}{m\pi b}\,\frac{\sinh\frac{m\pi b}{2a}(1-\frac{2y}{b})}{\cosh\frac{m\pi b}{2a}} \right\}$$

$$+ \sum_{m=1,3...} \frac{\pi^4 mb}{16a^3} l_m \cos\frac{m\pi x}{a}\left\{ \frac{\cosh\frac{m\pi y}{a}}{\sinh^2\frac{m\pi b}{2a}} + \frac{2y}{b}\,\frac{\sinh\frac{m\pi b}{2a}(1-\frac{2y}{b})}{\sinh\frac{m\pi b}{2a}} - \frac{2a}{m\pi b}\,\frac{\cosh\frac{m\pi b}{2a}(1-\frac{2y}{b})}{\sinh\frac{m\pi b}{2a}} \right\}$$

$$+ \sum_{n=1,2,3...} \frac{\pi^4 na}{16b^3} t_n \cos\frac{n\pi y}{b}\left\{ \frac{-\cosh\frac{n\pi x}{b}}{\cosh^2\frac{n\pi a}{2b}} + \frac{2x}{a}\,\frac{\cosh\frac{n\pi a}{2b}(1-\frac{2x}{a})}{\cosh\frac{n\pi a}{2b}} - \frac{2b}{n\pi a}\,\frac{\sinh\frac{n\pi a}{2b}(1-\frac{2x}{a})}{\cosh\frac{n\pi a}{2b}} \right\}$$

$$+ \sum_{m=1,3...} \frac{\pi^4}{16a^2} p_m \cos\frac{m\pi x}{a}\left\{ \frac{\sinh\frac{m\pi b}{a}(\frac{y}{b}-\frac{1}{2})}{\cosh^2\frac{m\pi b}{2a}} + \left(\frac{2y}{b}-1\right)\frac{\sinh\frac{m\pi b}{a}(1-\frac{y}{b})}{\cosh\frac{m\pi b}{2a}} \right\}$$

$$+ \sum_{m=1,3...} \frac{\pi^4 mb}{16a^3} S_m \frac{\cos\frac{m\pi x}{a}}{\sinh^2\frac{m\pi b}{2a}}\left\{ \left(\frac{y}{b}-\frac{1}{2}\right)\cosh\frac{m\pi b}{a}\left(\frac{3}{2}-\frac{y}{b}\right) + \left(\frac{3}{2}-\frac{y}{b}\right)\cosh\frac{m\pi b}{a}\left(\frac{y}{b}-\frac{1}{2}\right) \right.$$

$$\left. -\frac{a}{m\pi b}\sinh\frac{m\pi b}{a}\left(\frac{3}{2}-\frac{y}{b}\right) - \frac{a}{m\pi b}\sinh\frac{m\pi b}{a}\left(\frac{y}{b}-\frac{1}{2}\right) \right\}$$

$$\tag{11}$$

At the lower edge of the wall, it is desirable to know the vertical displacement v. This was found by substituting the value of ϕ from equation (6b) into

$$v = \frac{1}{E}\left(\int \frac{\delta^2 \phi}{\delta x^2}\, dy - \nu \frac{\delta \phi}{\delta y} \right) \qquad (12)$$

where E is Young's modulus, ν is Poisson's ratio, and the integration function has been taken as zero since it merely represents a rigid body rotation. The resulting expression for $(v)_{y=b/2}$ at the lower edge of the wall is

$$(v)_{y=b/2} = \frac{1+\nu}{E} \sum_{m=1,3\ldots} \frac{\pi^3 b}{160^2}\, l_m \sin \frac{m\pi x}{a} \left\{ \frac{\cosh \frac{m\pi b}{2a}}{\sinh^2 \frac{m\pi b}{2a}} + \frac{1-\nu}{1+\nu}\frac{2a}{m\pi b \sinh \frac{m\pi b}{2a}} \right\}$$

$$+ \frac{1}{E} \sum_{n=2,4\ldots} \frac{\pi^3 a}{16 b^2}\, t_n \cos \frac{n\pi}{2} \left[(1+\nu)\left\{ \frac{-\sinh \frac{n\pi x}{b}}{\cosh^2 \frac{n\pi a}{2b}} - \frac{2x}{a}\frac{\sinh \frac{n\pi a}{2b}\left(1-\frac{2x}{a}\right)}{\cosh \frac{n\pi a}{2b}} \right\} \right.$$

$$\left. + \frac{4b}{n\pi a}\frac{\cosh \frac{n\pi a}{2b}\left(1-\frac{2x}{a}\right)}{\cosh \frac{n\pi a}{2b}} \right]$$

$$+ \frac{1}{E} \sum_{m=1,3\ldots} \frac{\pi^2}{4m^2 b}\, P_m \sin \frac{m\pi x}{a}$$

$$+ \frac{1}{E} \sum_{m=1,3\ldots} \frac{\pi^3 b}{16 a^2}\, S_m \frac{\sin \frac{m\pi x}{a}}{\sinh^2 \frac{m\pi b}{2a}} \left\{ 1+\nu + \frac{a(1-\nu)}{m\pi b} \sinh \frac{m\pi b}{a} \right\}$$

$$(13)$$

The strain at the lower edge of the wall is found from the general equation

$$\epsilon_x = \frac{1}{E}\left(\sigma_x - \nu\sigma_y\right) = \frac{1}{E}\left(\frac{\partial^2\phi}{\partial y^2} - \nu\,\frac{\partial^2\phi}{\partial x^2}\right) \tag{14}$$

Substituting the value ϕ from equation (6b) into equation (14), the strain $(\epsilon_x)_{y=b/2}$ along the lower edge of the wall is,

$$(\epsilon_x)_{y=b/2} = \frac{1}{E}\sum_{m=1,3\ldots}\frac{\pi^4 m b}{16 a^3}\,k_m\,\sin\frac{m\pi x}{a}\left\{(1+\nu)\frac{\sinh\frac{m\pi b}{2a}}{\cosh^2\frac{m\pi b}{2a}} - \frac{4a}{m\pi b\,\cosh\frac{m\pi b}{2a}}\right\}$$

$$+\frac{1}{E}\sum_{n=1,3\ldots}\frac{\pi^4 n a}{16 b^3}\,t_n\,\sin\frac{n\pi}{2}\left[-(1+\nu)\left\{\frac{\sinh\frac{n\pi x}{b}}{\cosh^2\frac{n\pi a}{2b}} - \frac{2x}{a}\,\frac{\sinh\frac{n\pi a}{2b}\left(1-\frac{2x}{a}\right)}{\cosh\frac{n\pi a}{2b}}\right\}\right.$$

$$\left.+\,\frac{4\nu b\,\cosh\frac{n\pi a}{2b}\left(1-\frac{2x}{a}\right)}{n\pi a\,\cosh\frac{n\pi a}{2b}}\right]$$

$$+\frac{1}{E}\sum_{m=1,3\ldots}\frac{\pi^4}{16 a^2}\,P_m\,\sin\frac{m\pi x}{a}\left[\frac{-(1+\nu)}{\cosh^2\frac{m\pi b}{2a}} - \frac{2a(1-\nu)\,\sinh\frac{m\pi b}{2a}}{m\pi b\,\cosh\frac{m\pi b}{2a}}\right]$$

$$+\frac{1}{E}\sum_{m=1,3\ldots}\frac{-\pi^3}{4a^2}\,S_m\,\sin\frac{m\pi x}{a}$$

$$\tag{15}$$

The boundary conditions $(\sigma_x)_{x=0,a} = 0$, equation (3),

$(\sigma_y)_{y=b} = 0$, equation (2a), and $(\sigma_y)_{y=0} = 0$, equation (2b),

are automatically satisfied by the expressions used in either equations (6a) or (6b). Substituting the appropriate value

for $(\tau_{xy})_{y=b}$ in the second of equations (2a), expressing the

resulting equation as a Fourier series involving cosine terms, and equating the coefficients of the cosine terms to zero gives a set of equations involving k, ℓ, t, p, and s coefficients. Repeating the above process with the second of equations (2b) and combining the resulting equations with those obtained earlier gives

$$0 = \frac{\pi^2 b^2}{16 a^2}\left\{\frac{2a}{m\pi b}\tanh\frac{m\pi b}{2a} + \operatorname{sech}^2\frac{m\pi b}{2a}\right\}k_m + \frac{\pi^2 b}{16 ma}\tanh\frac{m\pi b}{2a}\operatorname{sech}\frac{m\pi b}{2a}\,p_m$$

$$+ \sum_{n\ odd}\frac{mn t_n}{\left(m^2\frac{b}{a}+n^2\frac{a}{b}\right)^2} \tag{16}$$

and,

$$0 = \frac{\pi^2 b^2}{32 a^2}\left\{\frac{2a}{m\pi b}\coth\frac{m\pi b}{2a} - \operatorname{cosech}^2\frac{m\pi b}{2a}\right\}\ell_m + \frac{\pi^2 b^2}{32 a^2}\left\{\frac{2a}{m\pi b}\operatorname{cosech}\frac{m\pi b}{2a}\right.$$

$$+ \frac{1}{1-\cosh\frac{m\pi b}{2a}} + \left.\operatorname{cosech}^2\frac{m\pi b}{2a}\right\}s_m + \sum_{n\ even}\frac{mn t_n}{2\left(m^2\frac{b}{a}+n^2\frac{a}{b}\right)^2}$$

$$\tag{17}$$

When the boundary condition in the second of equations
(3) is similarly used one obtains from those equations corres-
ponding to even cosine functions, n even,

$$O = \frac{\pi^2 a^2}{16 b^2}\left\{\frac{2b}{n\pi a}\tanh\frac{n\pi a}{2b} + \mathrm{sech}^2\frac{n\pi a}{2b}\right\}t_n + \sum_{m=1,3\ldots}\frac{mn\left\{\ell_m + (-1)^{\frac{n}{2}}s_m\right\}}{\left(m^2\frac{b}{a} + n^2\frac{a}{b}\right)^2}$$

$$(18)$$

and from those corresponding to odd cosine functions, n odd,

$$O = \frac{\pi^2 a^2}{16 b^2}\left\{\frac{2b}{n\pi a}\tanh\frac{n\pi a}{2b} + \mathrm{sech}^2\frac{n\pi a}{2b}\right\}t_n + \sum_{m=1,3\ldots}\frac{m\left\{nk_m + (-1)^{\frac{n-1}{2}}P_m\right\}}{\left(m^2\frac{b}{a} + n^2\frac{a}{b}\right)^2}$$

$$(19)$$

When the boundary condition in equation (4) is applied
and the resulting equation, including the constant term S/E,
is expressed as a Fourier series involving sine terms,
equating the coefficients of the successive sine terms to
zero gives

$$\frac{4S}{m\pi} = \frac{m\pi^4 b}{16 a^3}\left\{(1+\nu)\frac{\sinh\frac{m\pi b}{2a}}{\cosh^2\frac{m\pi b}{2a}} - \frac{4a}{m\pi b\cosh\frac{m\pi b}{2a}}\right\}k_m - \frac{\pi^3 S_m}{4a^2}$$

$$+ \sum_{n=1,3\ldots}\frac{(-1)^{\frac{n+1}{2}}\pi^2 m t_n\left(\frac{n^2}{b^2} - \frac{m^2\nu}{a^2}\right)}{\left(m^2\frac{b}{a} + n^2\frac{a}{b}\right)^2} + \frac{\pi^4}{16 a^2}\left\{\frac{-(1+\nu)}{\cosh^2\frac{m\pi b}{2a}} - \frac{2a(1-\nu)}{m\pi b}\tanh\frac{m\pi b}{2a}\right\}P_m$$

$$(20)$$

When boundary condition equation (5) is used with equation (13) and the coefficients of the successive sine terms are equated to zero one gets

$$0 = \frac{\pi^2}{4m^2 b} p_m + \frac{\pi^3 b}{16 a^2} \left\{ \frac{(1+\nu)\cosh\frac{m\pi b}{2a}}{\sinh^2\frac{m\pi b}{2a}} + \frac{2a(1-\nu)}{m\pi b \sinh\frac{m\pi b}{2a}} \right\} l_m$$

$$+ \frac{\pi^3 b}{16 a^3} \left\{ \frac{1+\nu}{\sinh^2\frac{m\pi b}{2a}} + \frac{2a(1-\nu)}{m\pi b} \coth\frac{m\pi b}{2a} \right\} s_m + \sum_{n=2,4\ldots} \frac{(-1)^{\frac{n}{2}} m n \pi \left(m^2 \frac{b}{a} - \nu n^2 \frac{a}{b}\right)}{na \left(m^2 \frac{b}{a} + n^2 \frac{a}{b}\right)^2}$$

It should be noted that each of equations (16) through (21) represents an infinite set of equations. With a finite number of coefficients, only a finite number of these equations can be satisfied. In the subsequent numerical solutions, we will include, starting with the lowest, as many of equations (16) as we have k coefficients, as many of equations (17) as l coefficients, as many of equations (18) as even t coefficients, as many of equations (19) as odd t coefficients, as many of equations (20) as s coefficients, and as many of equations (21) as p coefficients. The resulting solution, of course, will not satisfy the omitted equations and to that extent will not satisfy the given boundary conditions. By including a sufficient number of coefficients, however, the difference can be made quite small. A check on this point can readily be obtained by comparing a plot of the given boundary conditions with that of the boundary conditions satisfied. Where the difference is negligible from an engineering point of view, the solution is adequate.

3.4. Numerical examples

The computations were done both with conventional hand-computing machines and, where it seemed advisable, with SEAC, the NBS high speed electronic digital computer. SEAC was particularly useful in solving the large sets of simultaneous equations for the values of the coefficients.

Poisson's ratio has some effect on the answer because of the displacement boundary conditions at the bottom of the wall.

Experience with other related problems indicates that this effect should be small. In the solution given here the value $\nu = 0.3$ was used.

3.4.1. Wall with length twice height

For such a wall, $a = b$, two solutions were obtained. In the first of these, 9 coefficients were used - k_1, ℓ_1, t_1, t_2, p_1, p_3, s_1, s_3, and s_5. The corresponding nine equations are given in table 3 together with the values of the coefficients resulting from the solution. In the second solution, 40 coefficients were used. Their values are given in table 4.

The degree to which these solutions satisfy the given boundary conditions can be judged from figure 13, for the free boundaries $x = 0$, $x = a$, $y = b$, and from figure 14 for the restrained boundary, $y = b/2$. The agreement appears to be excellent for both solutions with the 40-term solution giving some superiority close to the corner attached to the footing. The agreement for the 40-term solution at distances from the corner exceeding 7 percent of the wall height is within 20 percent of the shrinkage strain S/E for the strain along the footing, within 3 percent of the shrinkage shortening Sa/E for the vertical displacement at the footing, and within 13 percent of the shrinkage stress S along the free walls.

The shearing stress in the wall at the footing for the 40-term solution is shown in figure 15. This stress is zero at the center, positive on the right half of the wall, and negative on the left half. In the center half of the wall, the stress varies nearly linearly. In the end quarters, the stress increases somewhat more rapidly and then in the last 10 percent of the wall length drops to a low value. The maximum shearing stress is less than $0.9S$.

The stresses at three locations near one corner of the wall are given in table 3 (a) for the 9-term solution and 3 (b) for the 40-term solution. The maximum stresses for the two solutions agree within 3 percent for the point at .0312a and within 1 percent for the points at .1403a and .2495a. The maximum shear stresses in the two solutions agree within 24 percent for the point at .0312a, within 20 percent for the point at .1403a, and within 7 percent for the point at .2495a. The directions of the maximum stresses agree within 29° for the point at .0312a, within 1° for the point at .1403a, and within 5° for the point at .2495a.

For all three points of the 40-term solution and for the two points farthest from the corner in the 9-term solution, the minimum stress is much smaller than the maximum stress in absolute value. In no case does the stress exceed the shrinkage stress S in magnitude. The maximum stress is directed approximately towards the bottom corner of the wall.

3.4.2. Wall with length twice height, non-uniform footing restraint

In the tests it was found that the strain along the footing was larger near the wall ends than it was at the center. This was attributed to the use in the tests of a finite ratio of footing cross-sectional area to wall cross-sectional area rather than the infinite ratio in equation (4). The distribution of $(\epsilon_x)_{y=b/2}$ in the test is shown in figure 16. The numerical solution with 40 coefficients is being repeated with boundary condition (4) replaced by the curve in figure 16. The computation is about one-half complete.

3.4.3. Wall with length and height equal

A numerical solution is being obtained for a wall whose length and width are equal, $b = 2a$. The solution makes use of 60 coefficients. The simultaneous equations for the coefficients have been coded for solution on SEAC. The work in this case is therefore about one half complete.

3.4.4. Wall with length four times height

The work on this wall has been started and is about 10 percent done.

REFERENCES

1. S. Timoshenko
   Theory of Elasticity
   McGraw-Hill Book Co., 1934.

Table 1.--Principal stresses in points A to G
Plaster Model No. 1 (Type I)

Point	$\dfrac{\sigma_x}{E \times \epsilon_m}$	$\dfrac{\sigma_y}{E \times \epsilon_m}$	$\dfrac{\tau_{xy}}{E \times \epsilon_m}$	$\alpha\ ^\circ$	$\dfrac{\sigma_{max}}{E \times \epsilon_m}$	$\dfrac{\sigma_{min}}{E \times \epsilon_m}$	$\alpha_1\ ^\circ$	$\dfrac{\tau_{max}}{E \times \epsilon_m}$
A	.445	.788	.656	51.3	1.290	-.066	6.3	.678
B	.946	.054	.459	22.9	1.138	-.142	-22.1	.641
C	.878	-.106	.280	14.8	.978	-.183	-30.2	.581
D	.013	.039	.064	51.0	.092	-.040	6.0	.066
E	.308	.149	.256	36.4	.496	-.042	- 8.6	.269
F	-.012	-.077	-.005	85.1	-.012	-.077	40.1	.033
G	.219	.050	.100	23.4	.265	.002	-21.6	.131

Table 2.--Comparison of computed and experimental values
Plaster Model No. 1 (Type 1)

Point	Method of determin.	$\dfrac{\sigma_x}{E \times \epsilon_m}$	$\dfrac{\sigma_y}{E \times \epsilon_m}$	$\dfrac{\tau_{xy}}{E \times \epsilon_m}$	α°	$\dfrac{\sigma_{max}}{E \times \epsilon_m}$	$\dfrac{\sigma_{min}}{E \times \epsilon_m}$	$\alpha_1^{\,\circ}$	$\dfrac{\tau_{max}}{E \times \epsilon_m}$
A	9-term solution	.256	.393	.465	49.19	.794	-.145	4.19	.470
A	40-term solution	.042	.733	.160	77.56	.769	.006	32.56	.381
A	Experim.	.445	.788	.656	51.30	1.290	-.066	6.30	.678
E	9-term solution	.269	.184	.197	38.96	.428	.025	- 6.04	.202
E	40-term solution	.230	.139	.237	39.59	.426	-.057	- 5.41	.241
E	Experim.	.308	.149	.256	36.40	.496	-.042	- 8.60	.269
G	9-term solution	.183	.059	.087	27.31	.228	.014	-17.69	.107
G	40-term solution	.194	.036	.082	23.10	.229	.001	-21.90	.114
G	Experim.	.219	.050	.100	23.40	.265	.002	-21.60	.131

Table 3.--Wall with length twice height, first solution, 9
         coefficients.

EQUATIONS

$$0 = 0.458139k_1 + 0.25t_1 + .225470p_1$$

$$0 = 0.25k_1 + 0.458139t_1 + 0.25p_1 + 0.03p_3$$

$$0 = 2.467401p_1 + 1.568861\ell_1 + 0.012566t_2 + 1.417290s_1$$

$$0 = 0.274156p_3 - 0.217495t_2 - 0.288723s_3$$

$$0 = 0.155848\ell_1 + 0.04t_2 - 0.060807s_1$$

$$0 = 0.08\ell_1 + 0.200208t_2 - 0.08s_1 - 0.035503s_3 - 0.011891s_5$$

$$1.273240Sa^2 = - 0.196395k_1 - 1.727181t_1 - 3.745349p_1 - 7.751569s_1$$

$$0.424413Sa^2 = 0.503350t_1 - 1.046393p_3 - 7.751569s_3$$

$$0.254648Sa^2 = 0.474500t_1 - 7.751569s_5$$

SOLUTION

$$k_1/Sa^2 = -0.049880 \qquad\qquad p_1/Sa^2 = 0.180376$$

$$\ell_1/Sa^2 = -0.071428 \qquad\qquad p_3/Sa^2 = 0.000905$$

$$t_1/Sa^2 = -0.071269 \qquad\qquad s_1/Sa^2 = -0.234265$$

$$t_2/Sa^2 = -0.077826 \qquad\qquad s_3/Sa^2 = -0.059486$$

$$s_5/Sa^2 = -0.037214$$

Remaining coefficients taken as zero.

Table 4.--Wall with length twice height, second solution, 40
coefficients.

$k_1/Sa^2 = -.059389251$ $t_{10}/Sa^2 = -.011612346$

$k_3/Sa^2 = .012303806$ $t_{12}/Sa^2 = .008939071$

$k_5/Sa^2 = .003772472$ $t_{14}/Sa^2 = -.005983598$

$k_7/Sa^2 = .001304913$ $t_{16}/Sa^2 = .004767099$

$\ell_1/Sa^2 = -.075968510$ $p_1/Sa^2 = .188439011$

$\ell_3/Sa^2 = .010713538$ $p_3/Sa^2 = -.003551489$

$\ell_5/Sa^2 = .005101076$ $p_5/Sa^2 = -.163158134$

$\ell_7/Sa^2 = .001912432$ $p_7/Sa^2 = -.354676034$

$t_1/Sa^2 = -.061716726$ $p_9/Sa^2 = -.555787489$

$t_3/Sa^2 = -.000280045$ $p_{11}/Sa^2 = -.759714680$

$t_5/Sa^2 = .027934929$ $p_{13}/Sa^2 = -.963912395$

$t_7/Sa^2 = -.024216724$ $p_{15}/Sa^2 = -1.167365113$

$t_9/Sa^2 = .022785816$ $s_1/Sa^2 = -.242707516$

$t_{11}/Sa^2 = -.018657394$ $s_3/Sa^2 = -.063090690$

$t_{13}/Sa^2 = .015630606$ $s_5/Sa^2 = -.029900727$

$t_{15}/Sa^2 = -.012683033$ $s_7/Sa^2 = -.012157563$

$t_2/Sa^2 = -.082028509$ $s_9/Sa^2 = -.001303778$

$t_4/Sa^2 = .059449535$ $s_{11}/Sa^2 = .005902147$

$t_6/Sa^2 = -.025981647$ $s_{13}/Sa^2 = .010951224$

$t_8/Sa^2 = .019490944$ $s_{15}/Sa^2 = .014630406$

Remaining coefficients taken as zero.

Table 5.--Stresses at three locations near corner

(a) 9-term solution

Location		Stresses			Principal stresses				Maximum shear	
					Maximum		Minimum			
x/a	$y/a-1/2$	σ_x/s	σ_y/s	τ_{xy}/s	σ/s	α_i,*°	σ/s	α_i,°	τ/s	α_i,°
.0312	.0312	.256	.393	.465	.794	49.19	-.145	-40.81	.470	4.19
.1403	.1403	.269	.184	.197	.428	38.96	.0245	-51.04	.202	-6.04
.2495	.2495	.183	.0590	.0872	.228	27.31	.0140	-62.69	.107	-17.69

(b) 40-term solution

Location		Stresses			Principal stresses				Maximum shear	
					Maximum		Minimum			
x/a	$y/a-1/2$	σ_x/s	σ_y/s	τ_{xy}/s	σ/s	α_i,°	σ/s	α_i,°	τ/s	α_i,°
.0312	.0312	.0415	.733	.160	.769	77.56	.00606	-12.44	.381	32.56
.1403	.1403	.230	.139	.237	.426	39.59	-.0566	-50.41	.241	-5.41
.2495	.2495	.194	.0357	.0823	.229	23.10	.000552	-66.90	.114	-21.90

*Angle α, measured positively from x-axis counterclockwise, figure 1.

16"

12"

t

4¼"

1¼"

32"
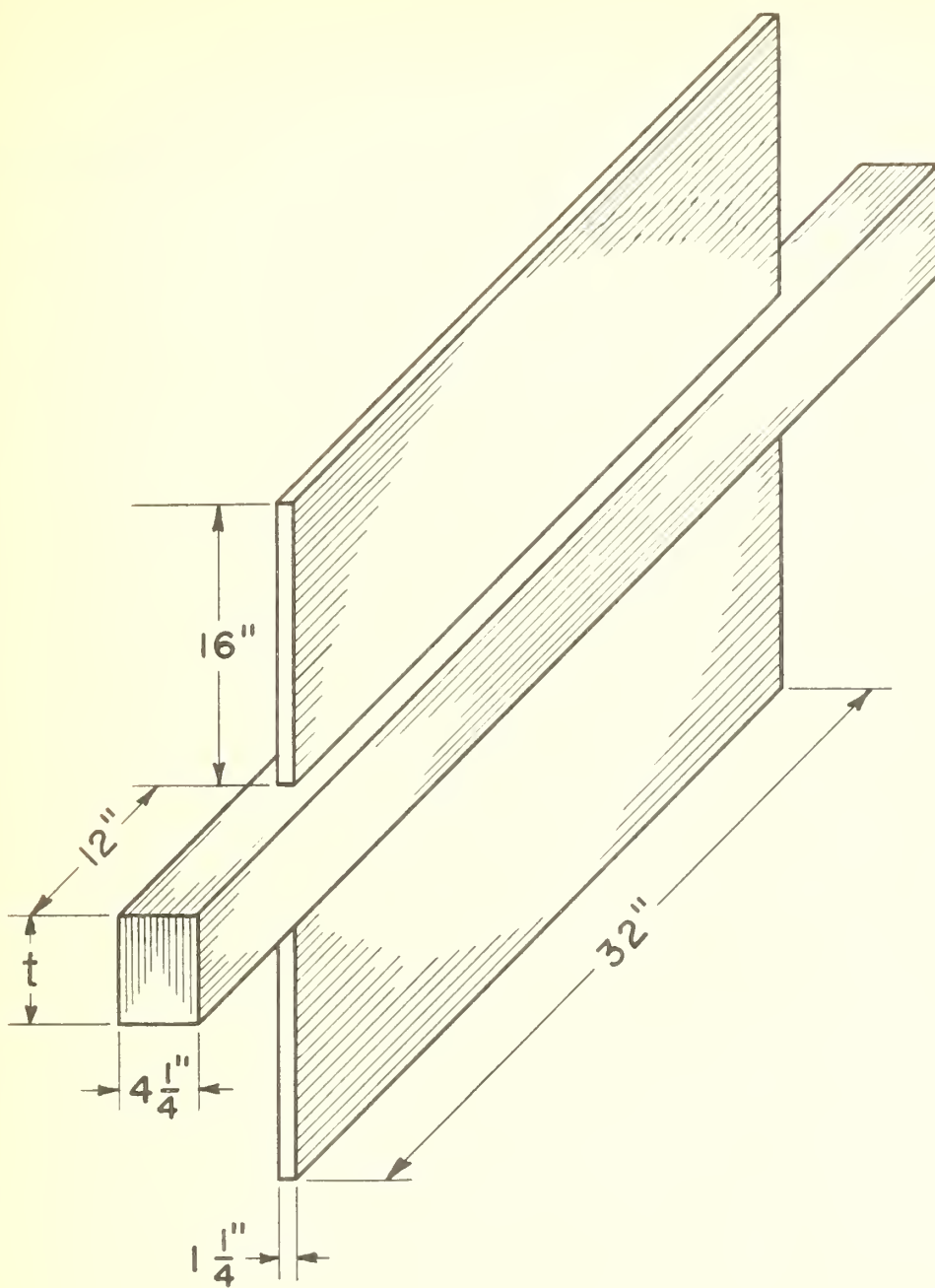
TYPE I: $t = 3\frac{1}{2}''$

TYPE II: $t = 6\frac{1}{4}''$

FIG. 1   DIMENSIONS AND FORM OF WALL MODELS

0% RESTRAINT

a. FREE SHRINKAGE

100% RESTRAINT

b. RESTRAINED SHRINKAGE

100% RESTRAINT
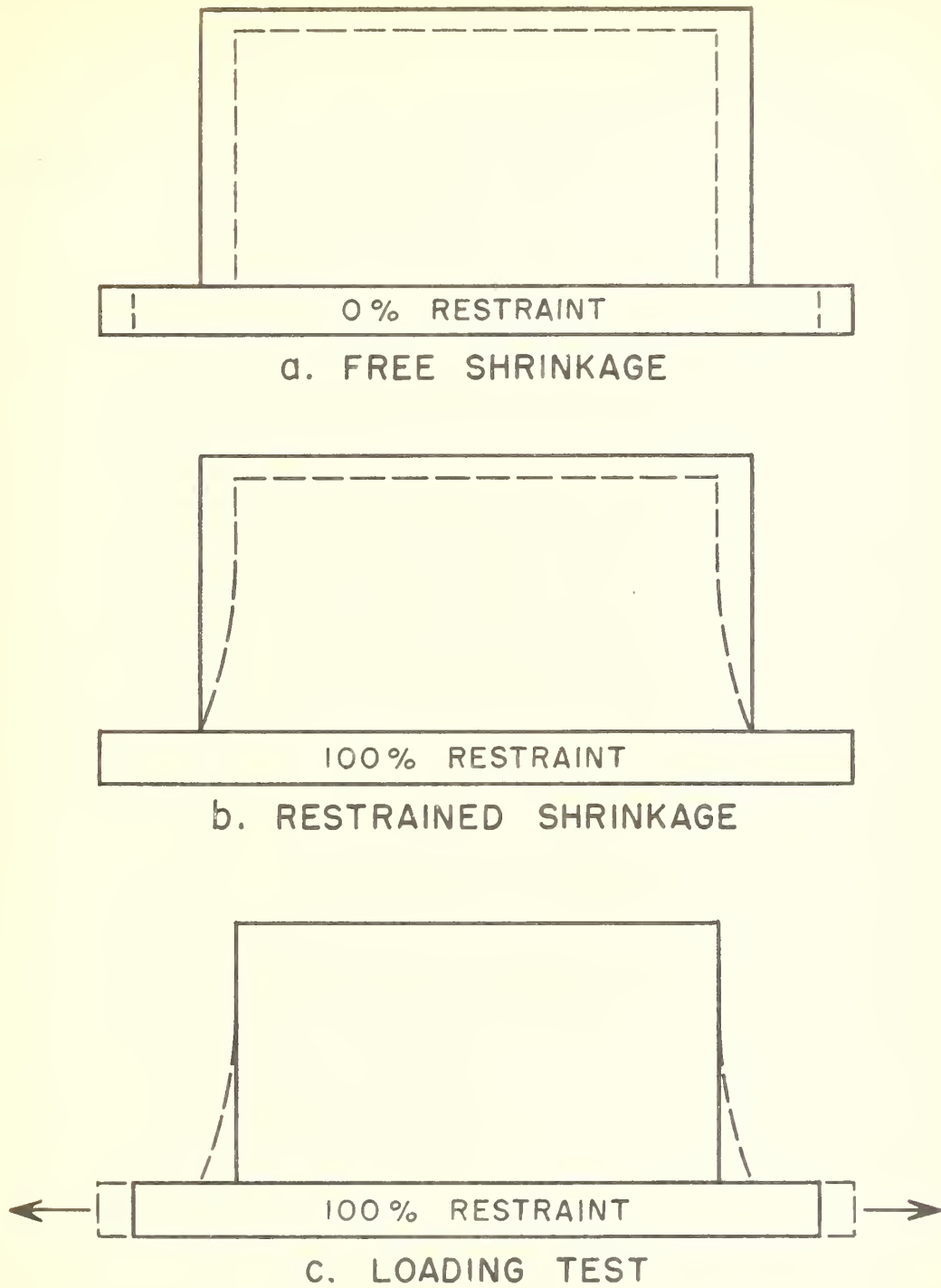
c. LOADING TEST

FIG. 2 ANALOGY OF LOADING TEST TO RESTRAINED SHRINKAGE
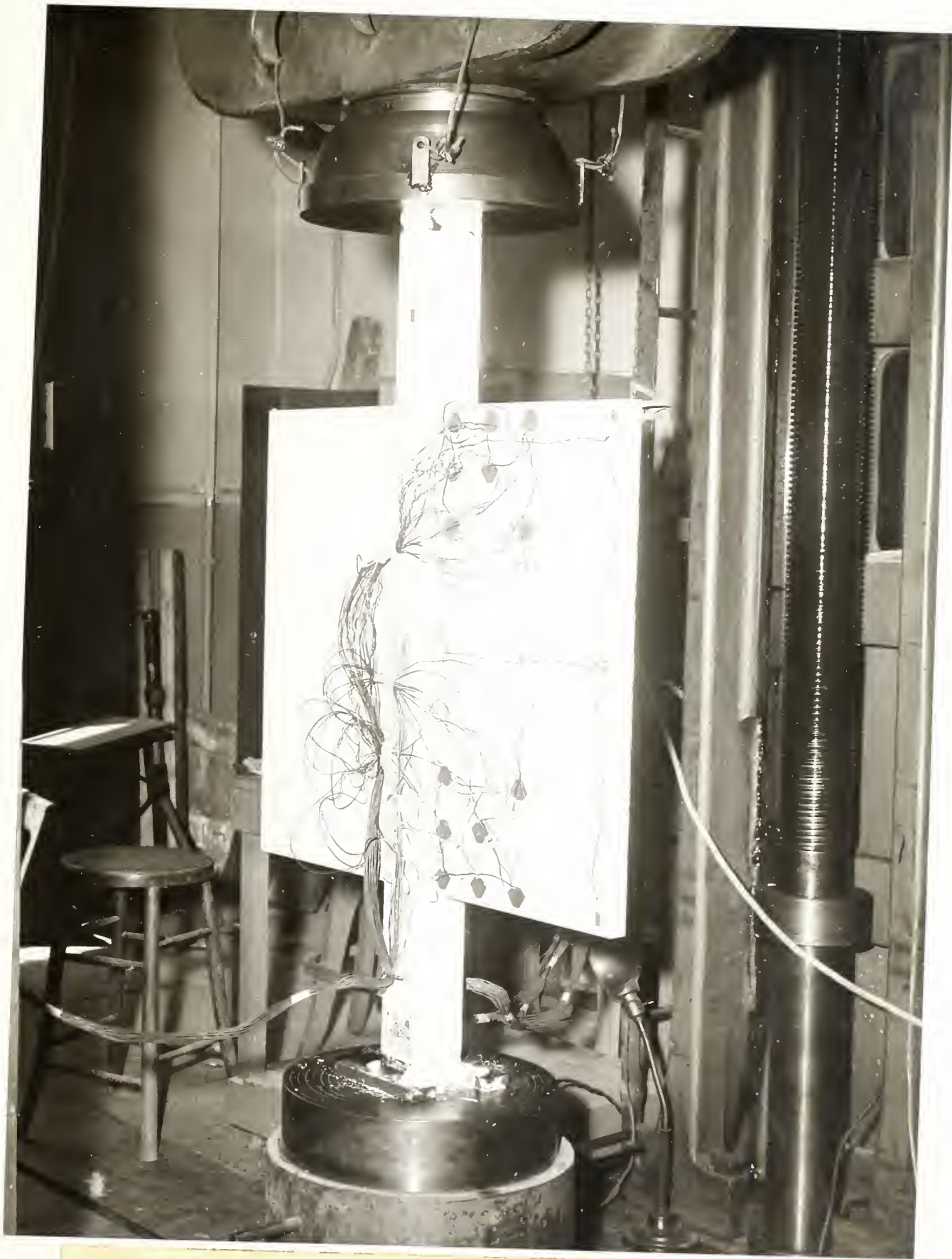
Fig. 3 - A plaster model with gages in a testing machine

FIG. 4 STRAIN GAGES ON PLASTER MODEL NO.1 (TYPE I)
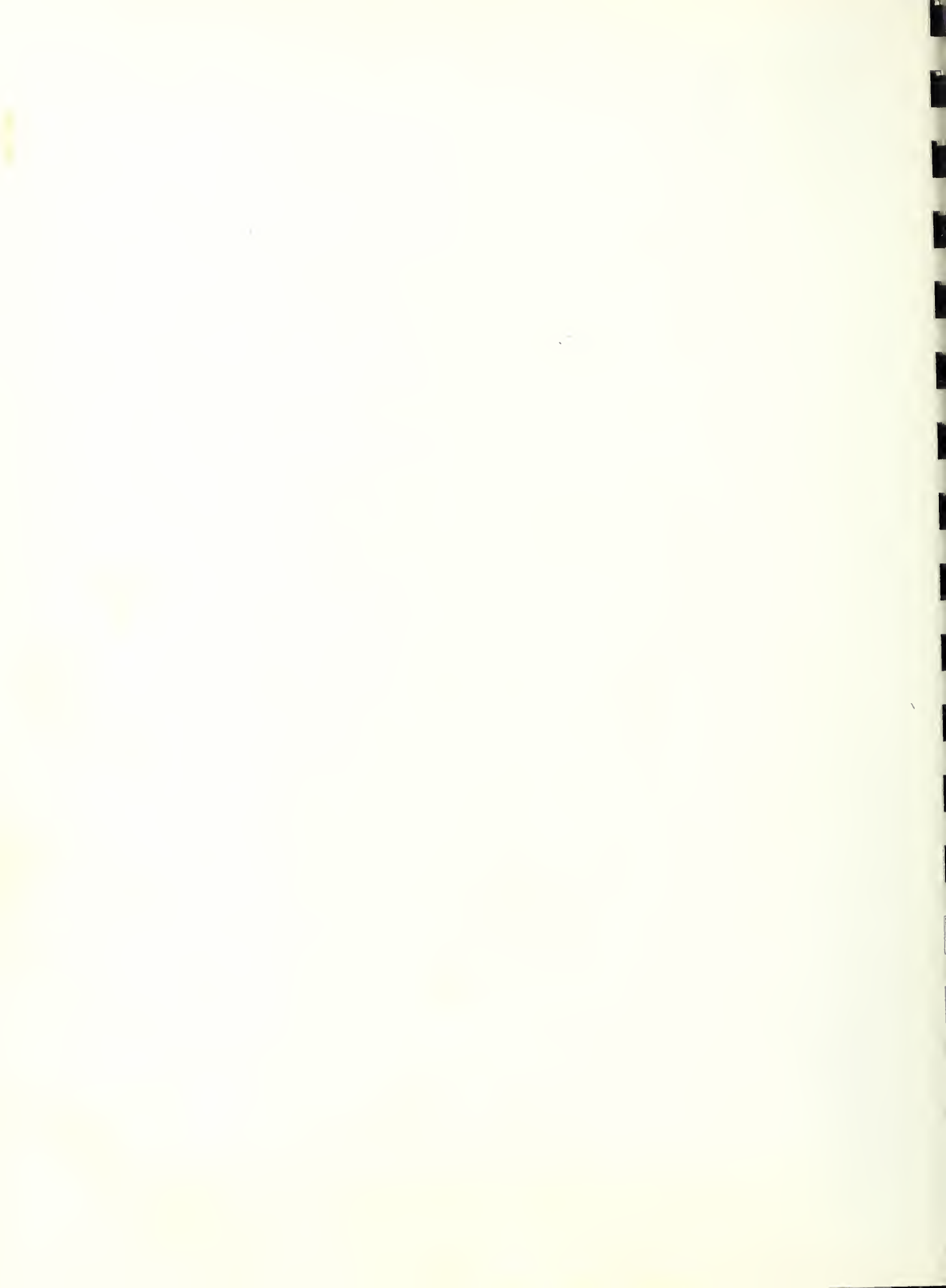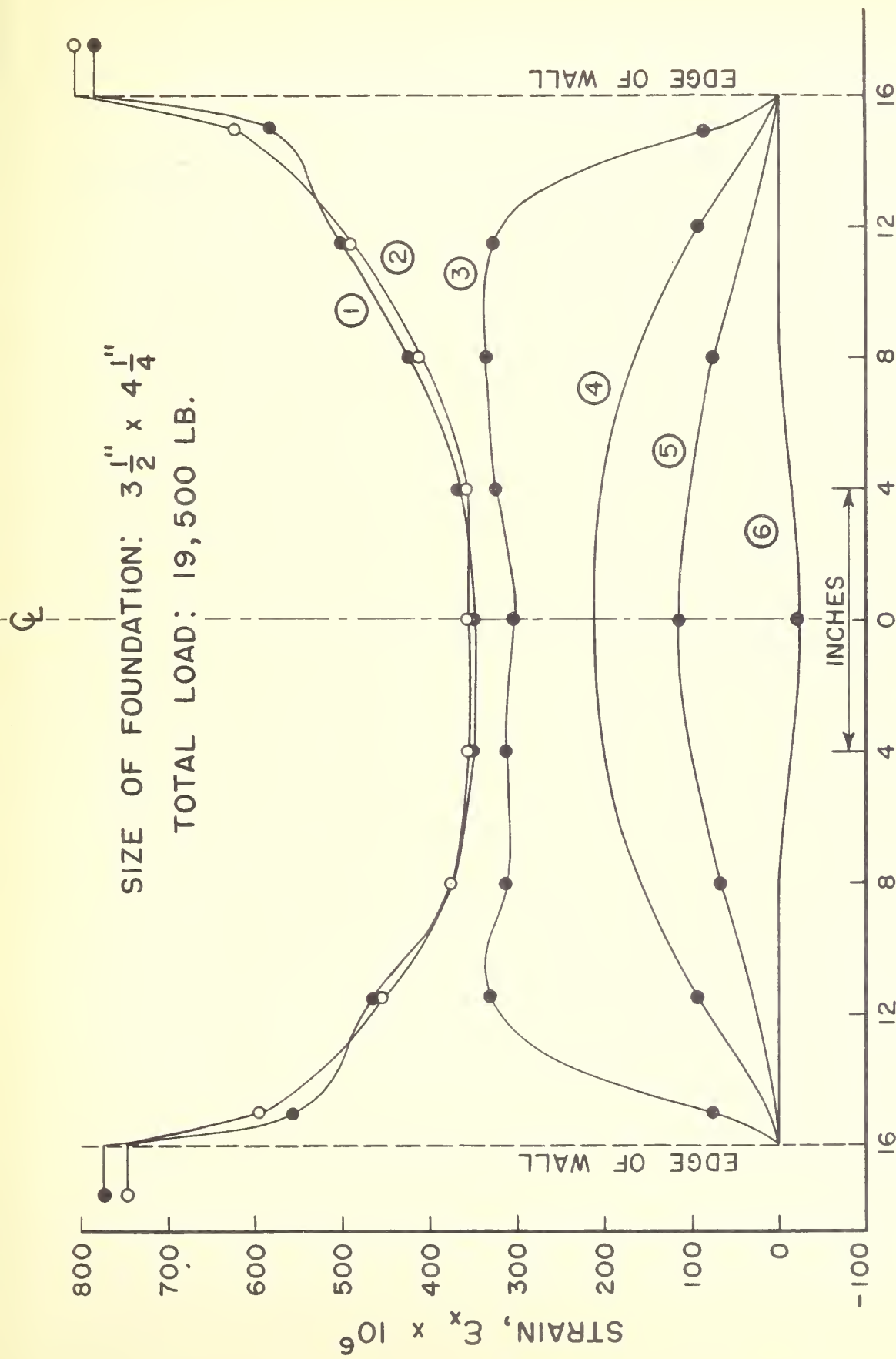
FIG. 5   HORIZONTAL STRAINS IN PLASTER MODEL NO. I (TYPE I)

NOTE: ENCIRCLED NUMBERS REFER TO WALL LEVELS IN FIG. 4
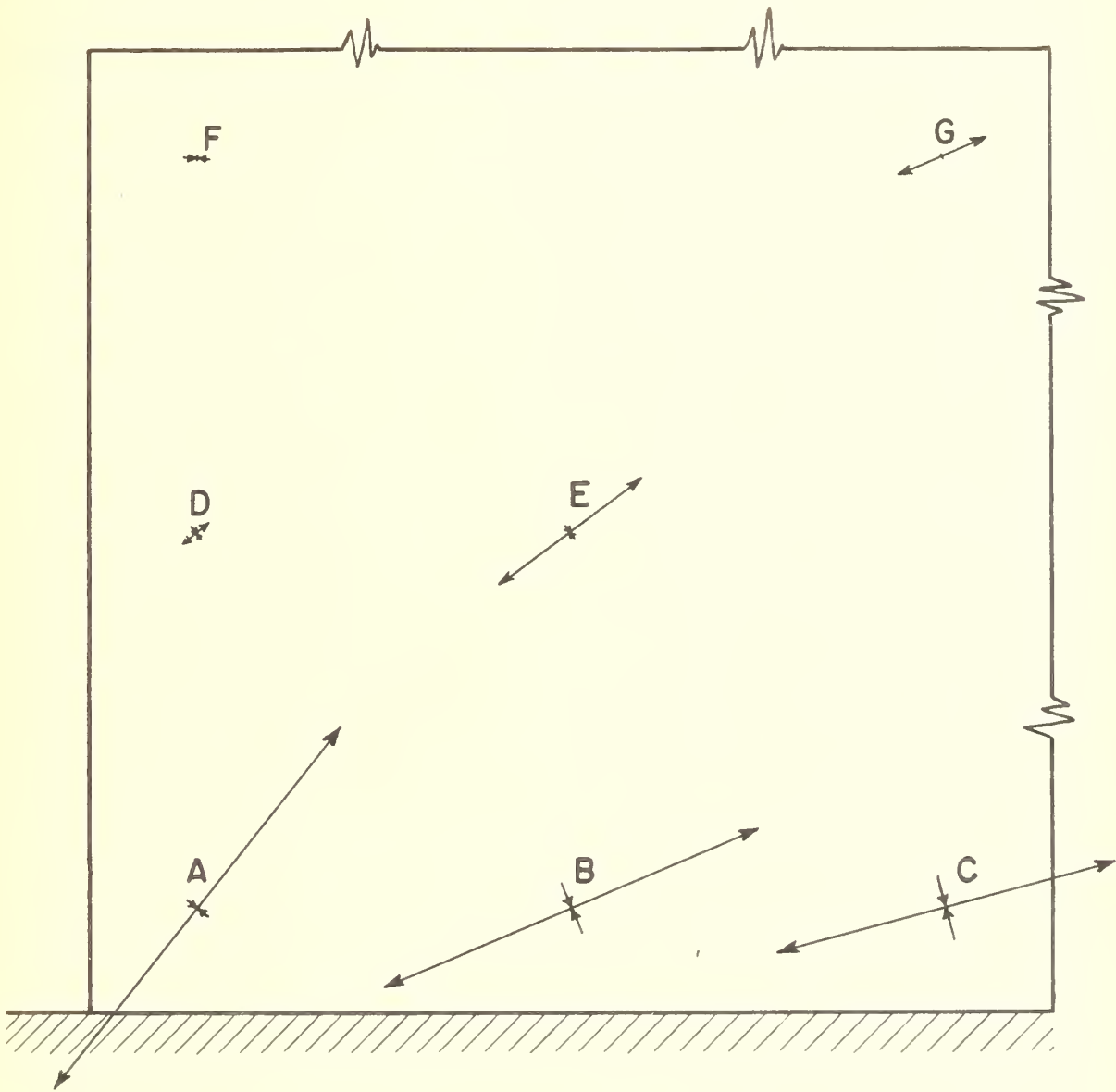
FIG. 6 PRINCIPAL STRESSES IN PLASTER MODEL NO. I (TYPE I)
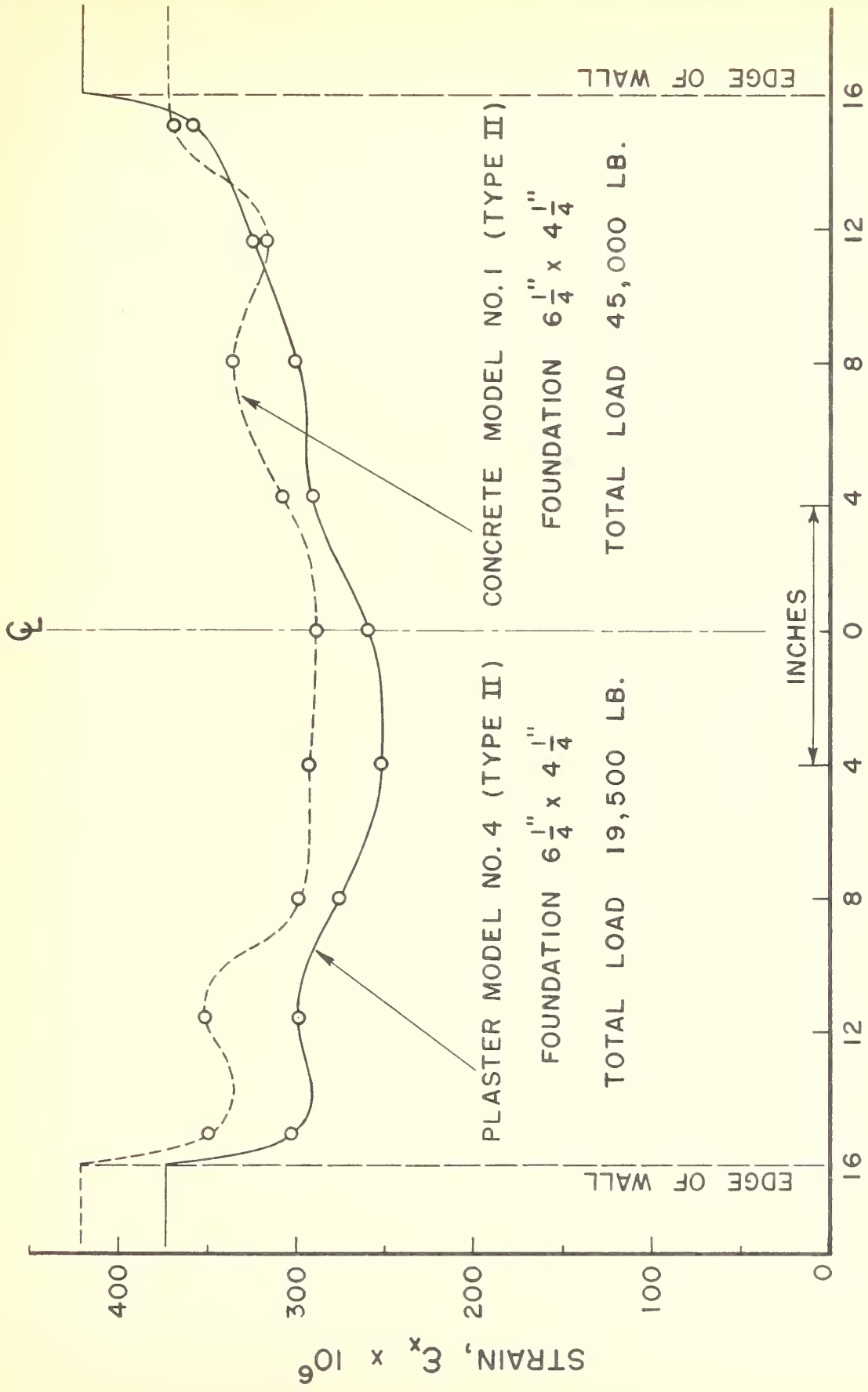
FIG. 7 HORIZONTAL STRAIN IN FOUNDATION
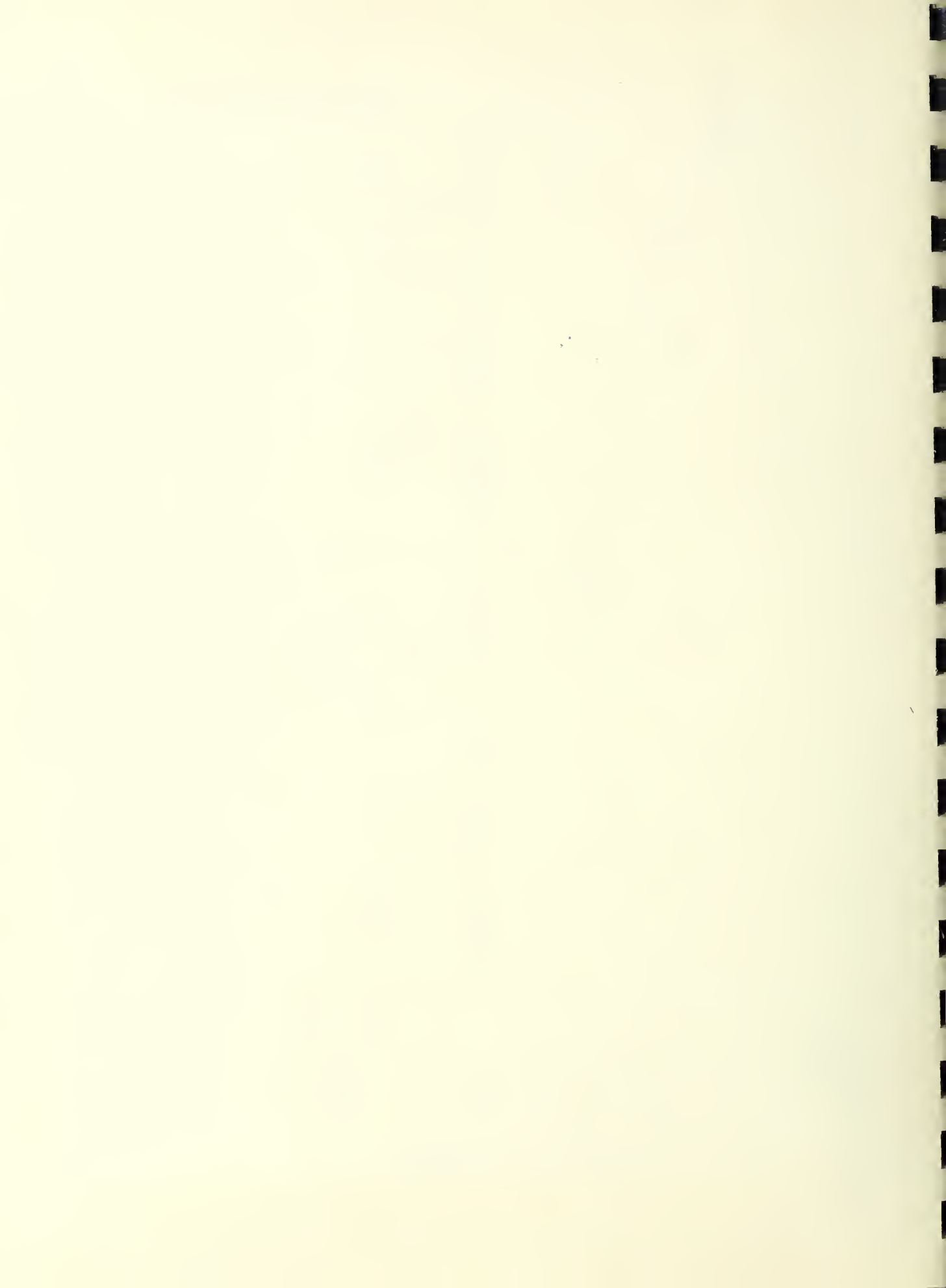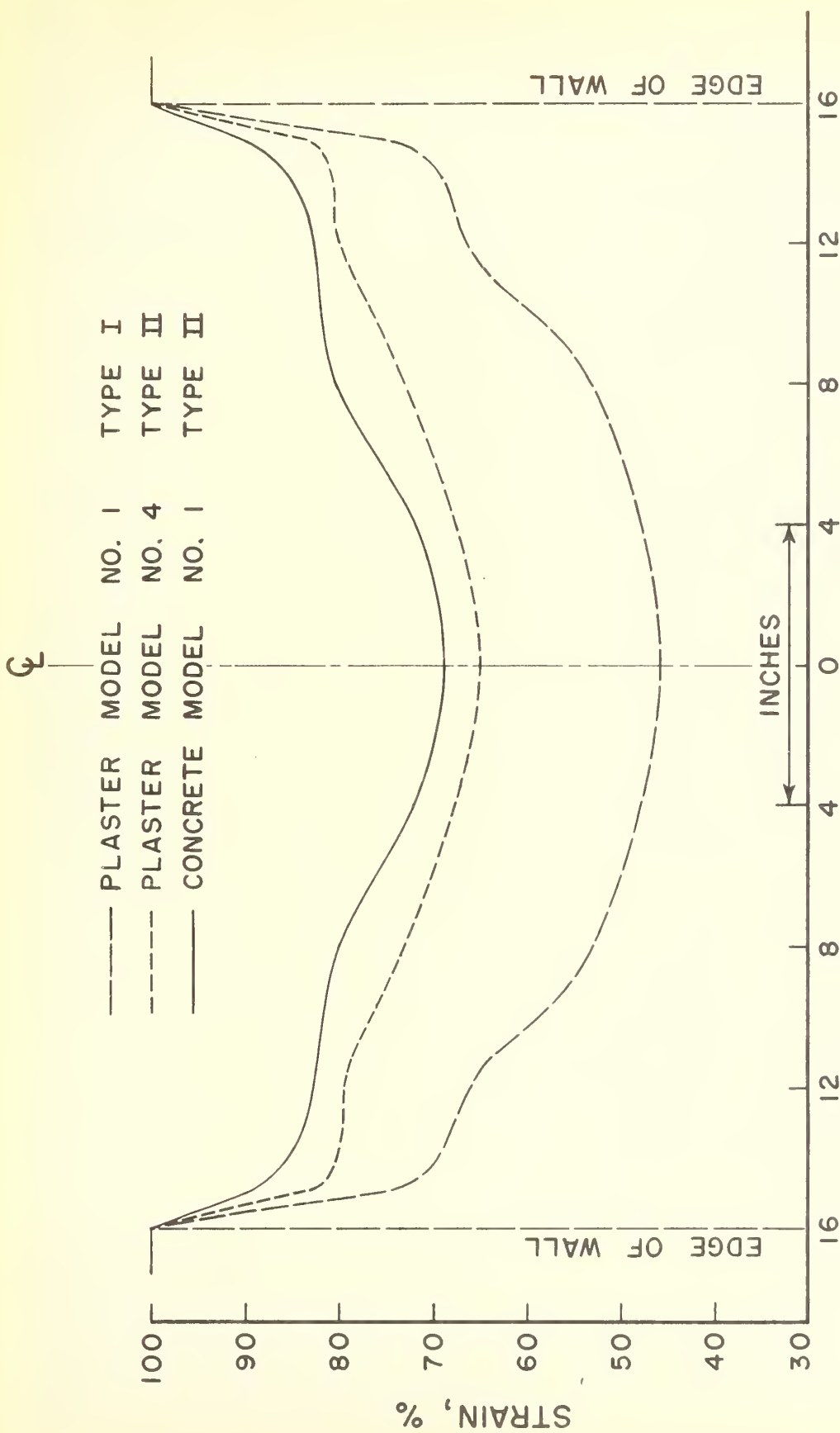
FIG. 8 HORIZONTAL STRAIN IN FOUNDATION EXPRESSED AS PERCENTAGE OF THAT AT FREE ENDS. RESULTS AVERAGED WITH RESPECT TO CENTER LINE.
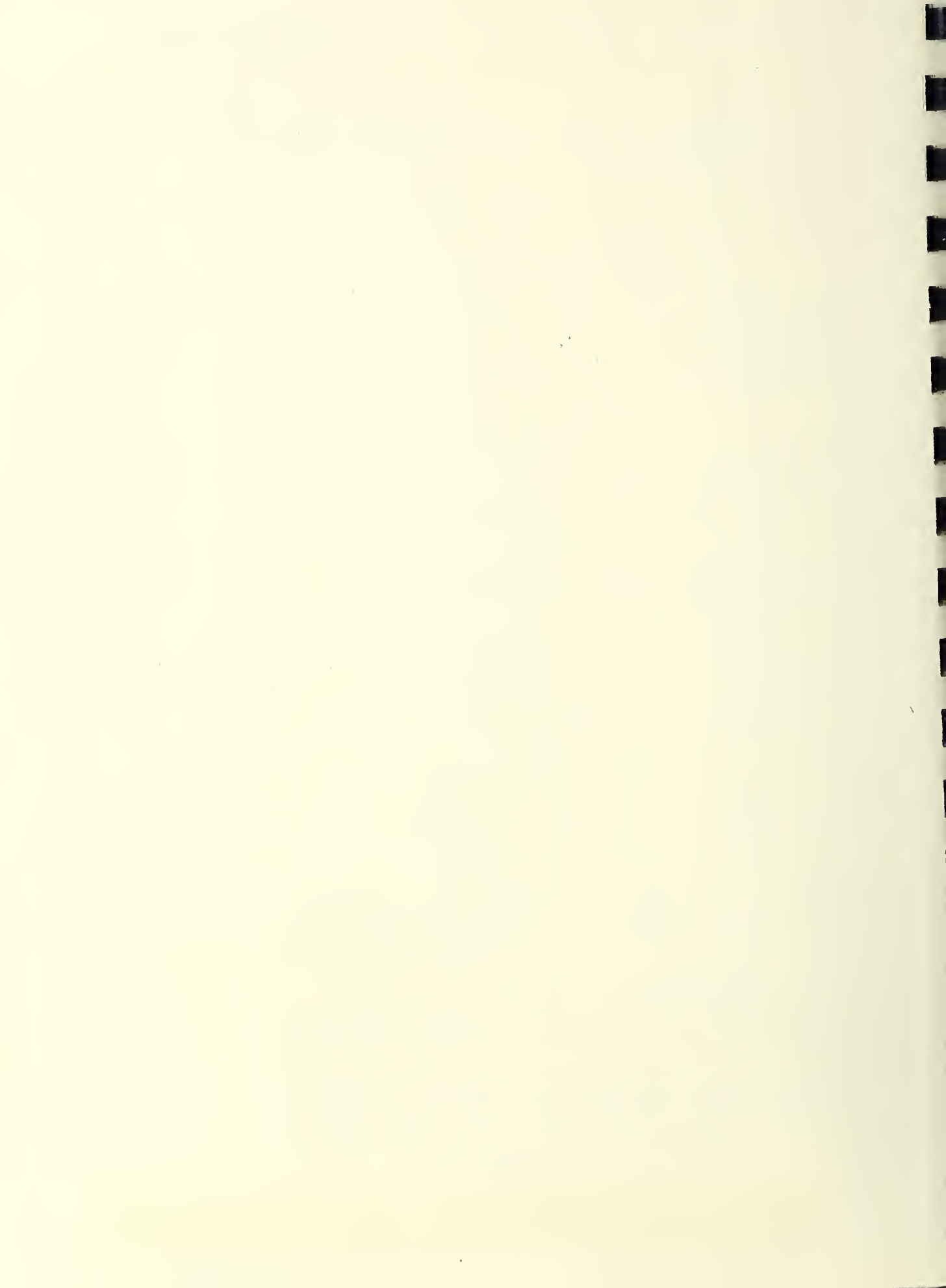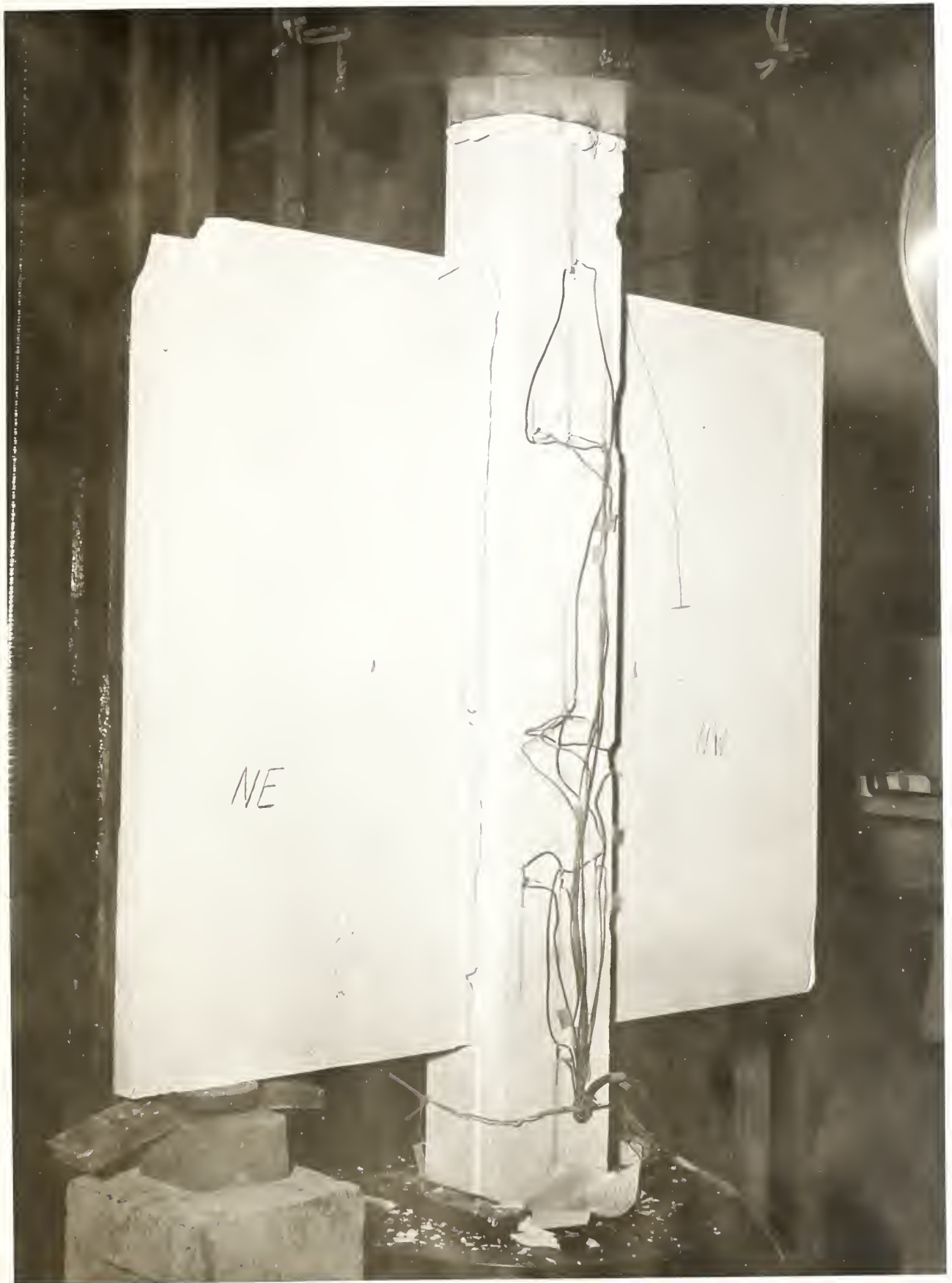
Fig. 9 - View of plaster model of type II showing the
crack pattern developed in a compression test.

a. COMPUTED VALUES. 9 - TERM SOLUTION.
b. COMPUTED VALUES. 40 - TERM SOLUTION.
c. EXPERIMENTAL VALUES.
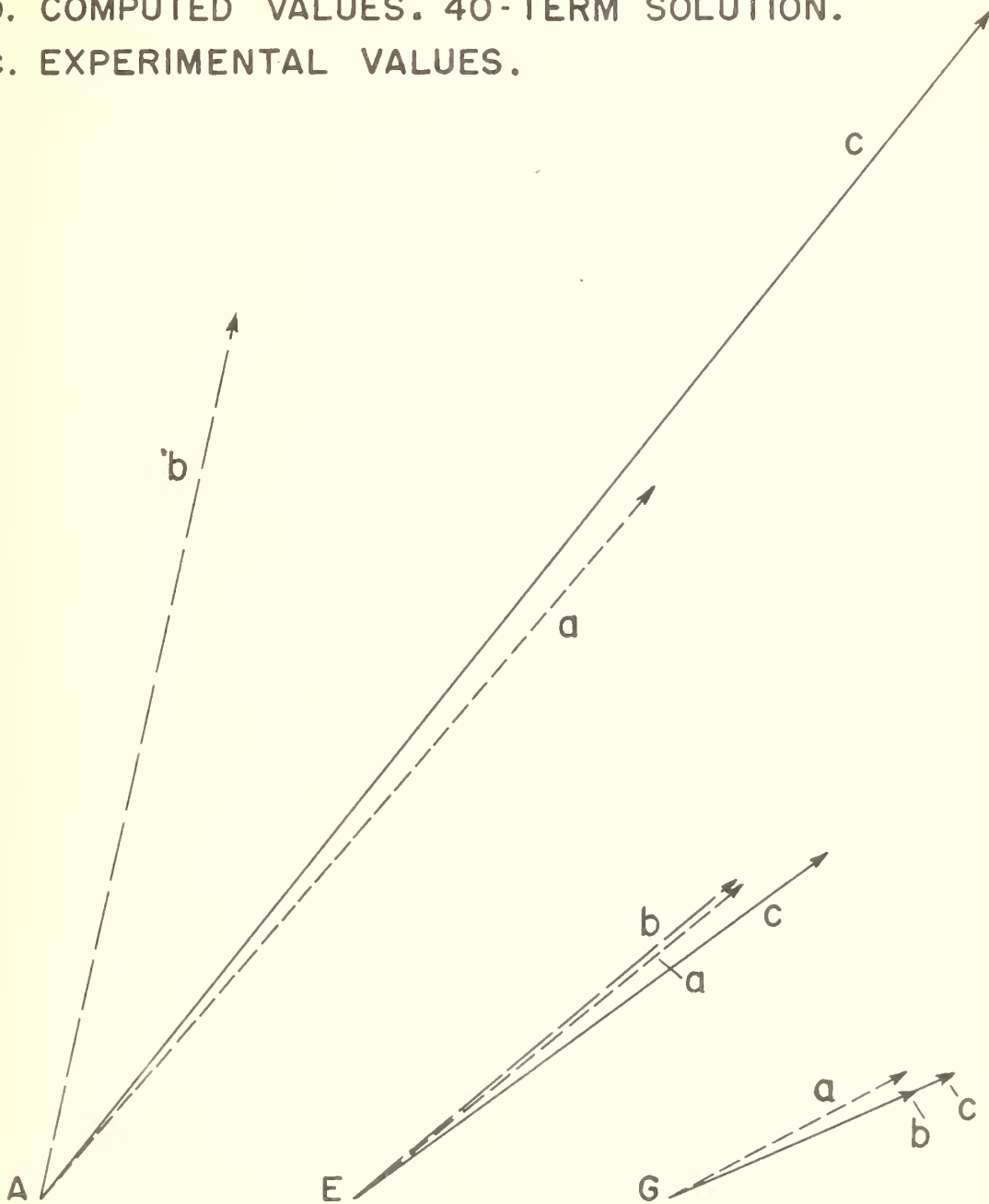
FIG. 10 COMPARISON OF COMPUTED AND EXPERIMENTAL VALUES
OF PRINCIPAL STRESSES AT POINTS A, E, AND G.
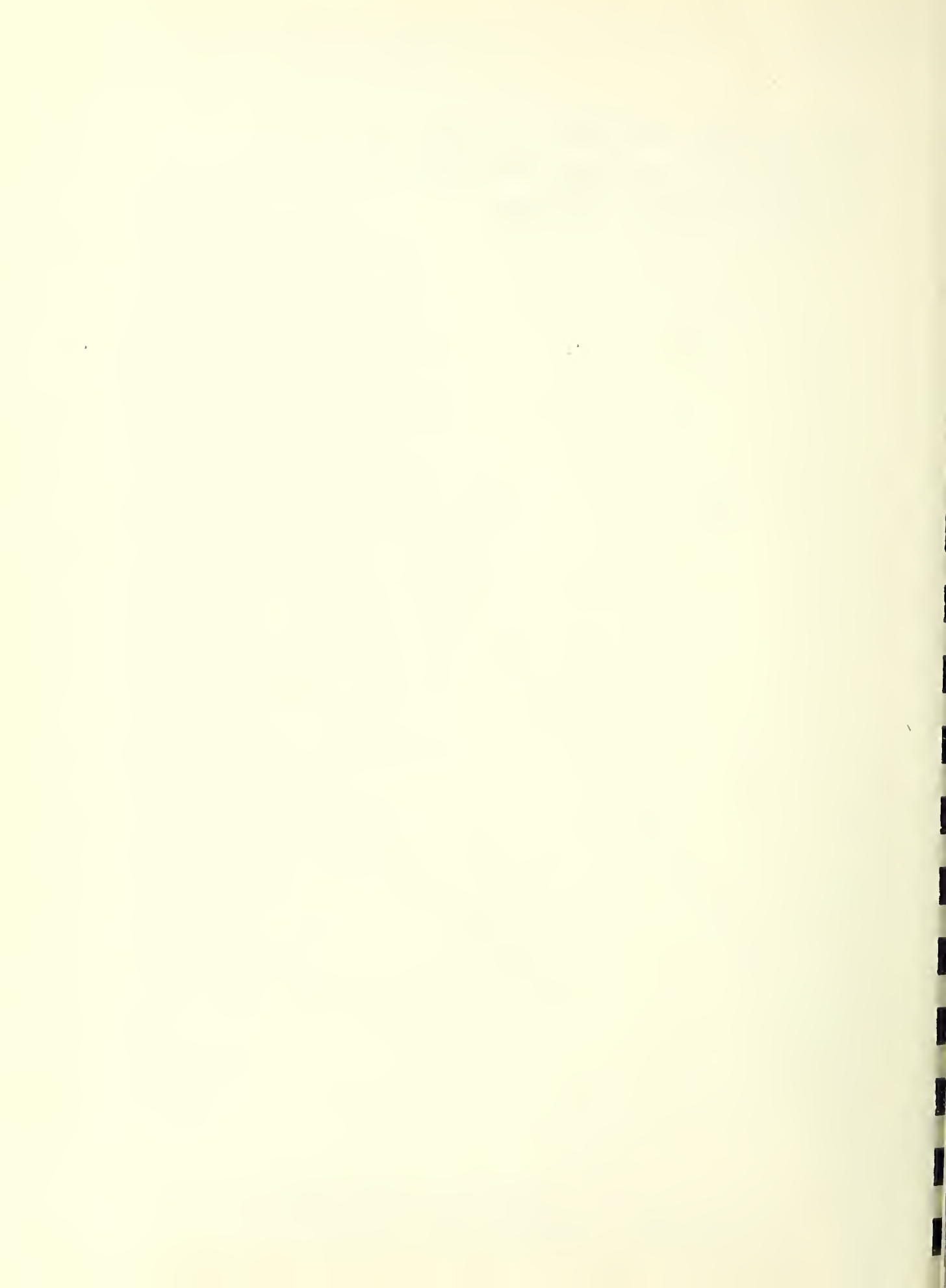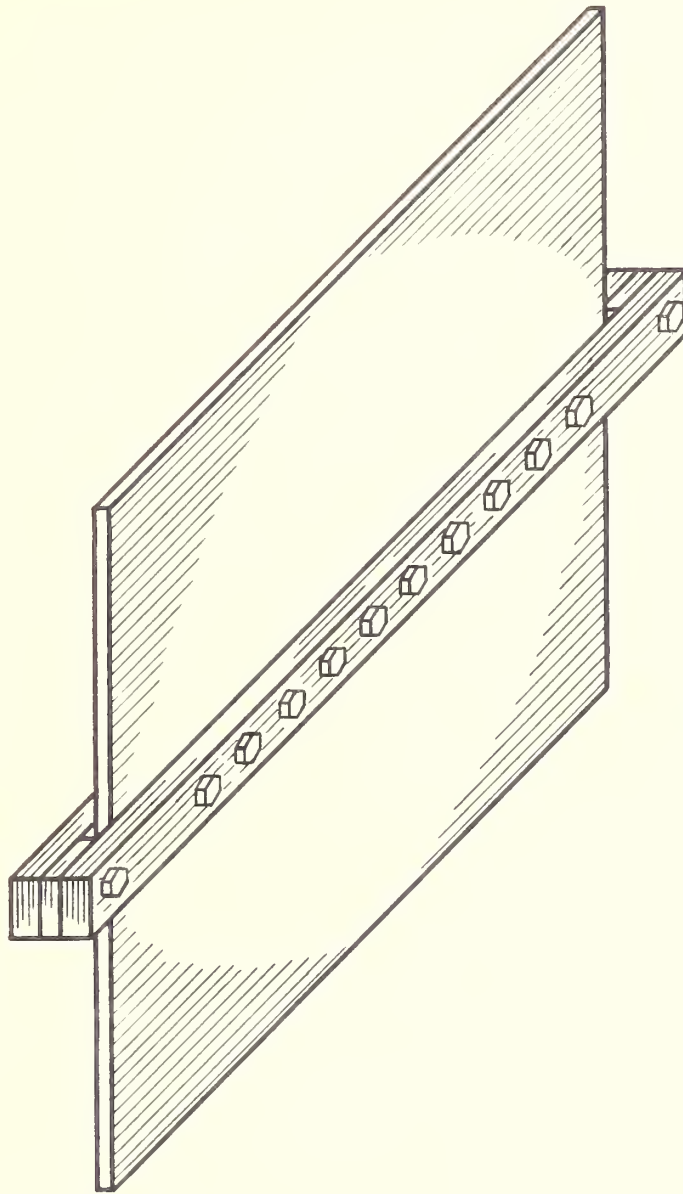
FIG. 11   WALL MODELS WITH STEEL FOUNDATION
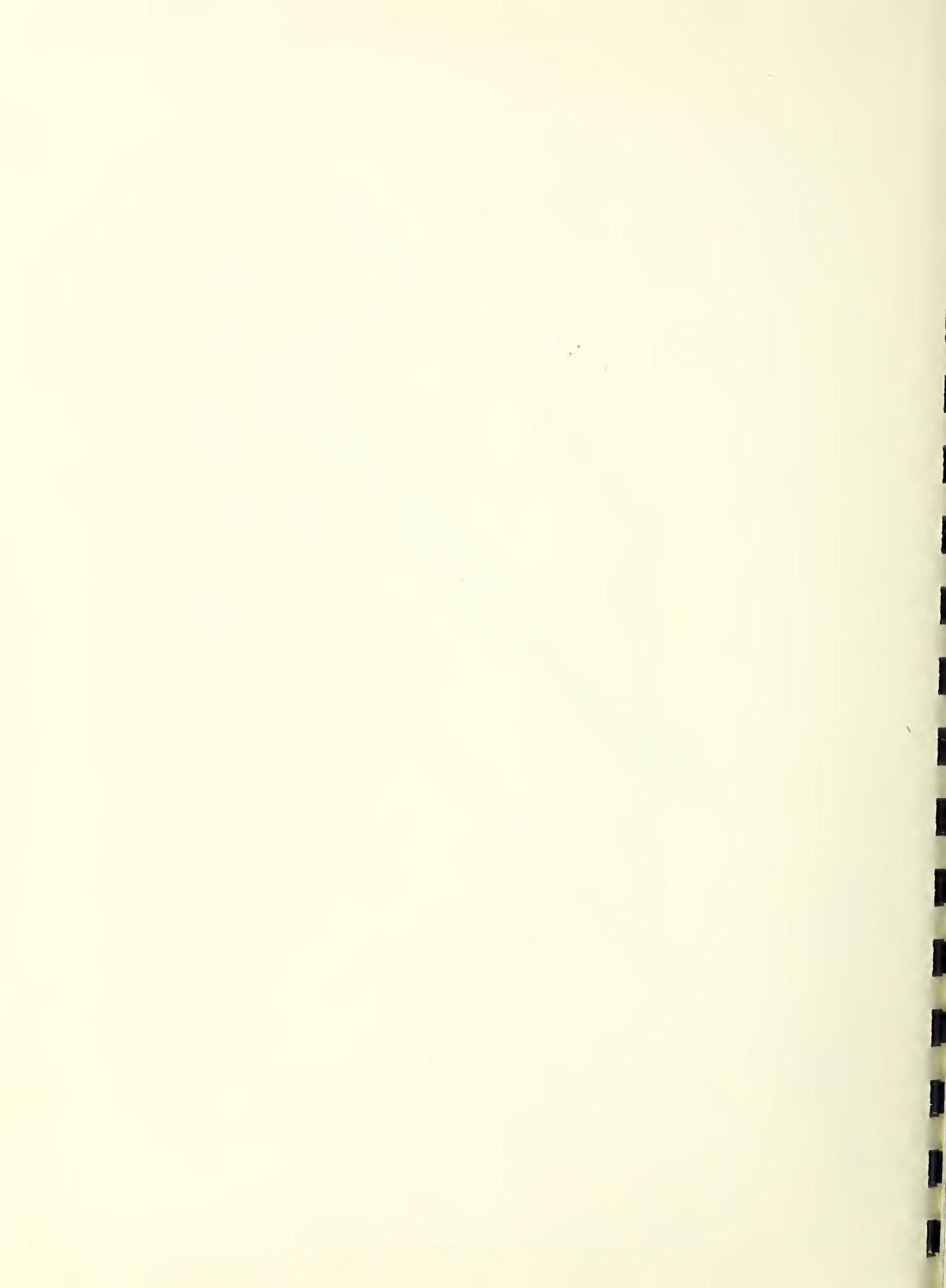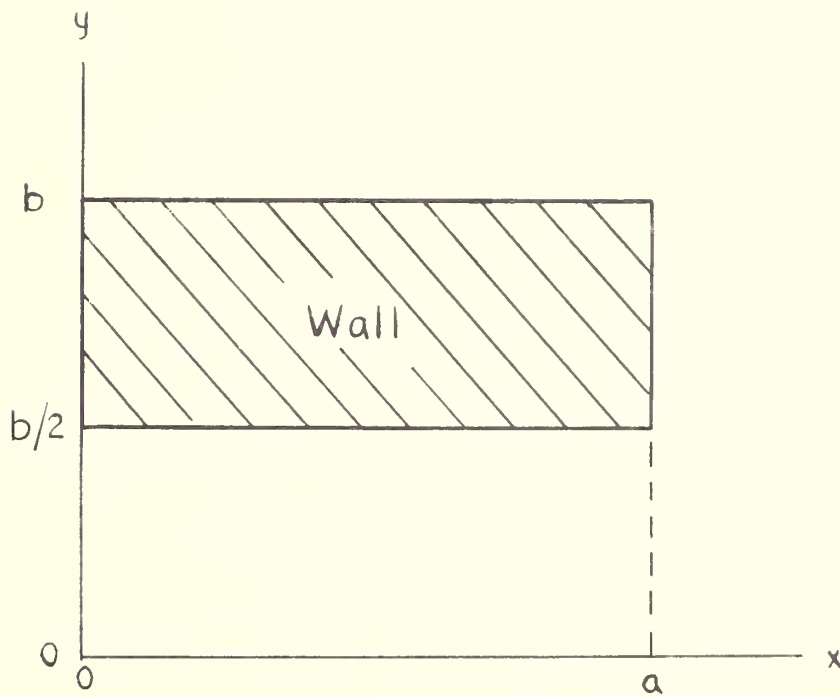
Fig. 12 – Coordinate system for theoretical analysis. Top of wall along $y = b$, bottom along $y = b/2$, one side along $x = 0$, and the other along $x = a$.
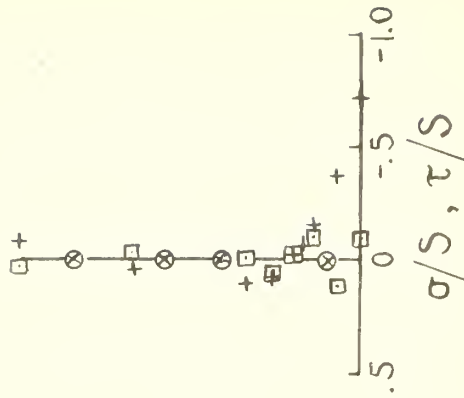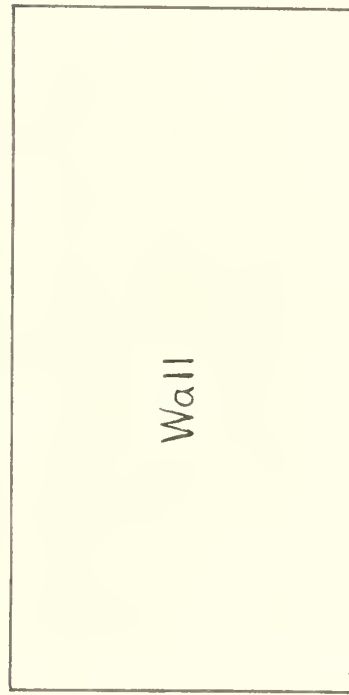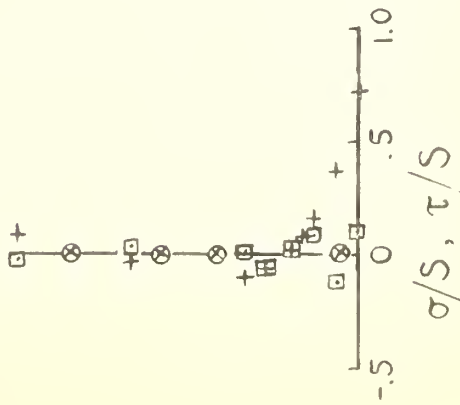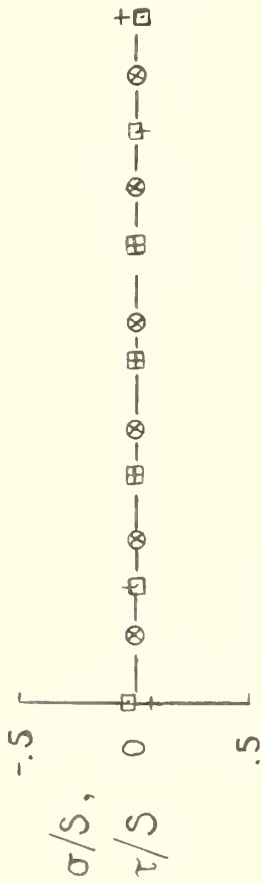
Fig. 13 – Agreement of boundary values in solutions with given boundary conditions along free edges.
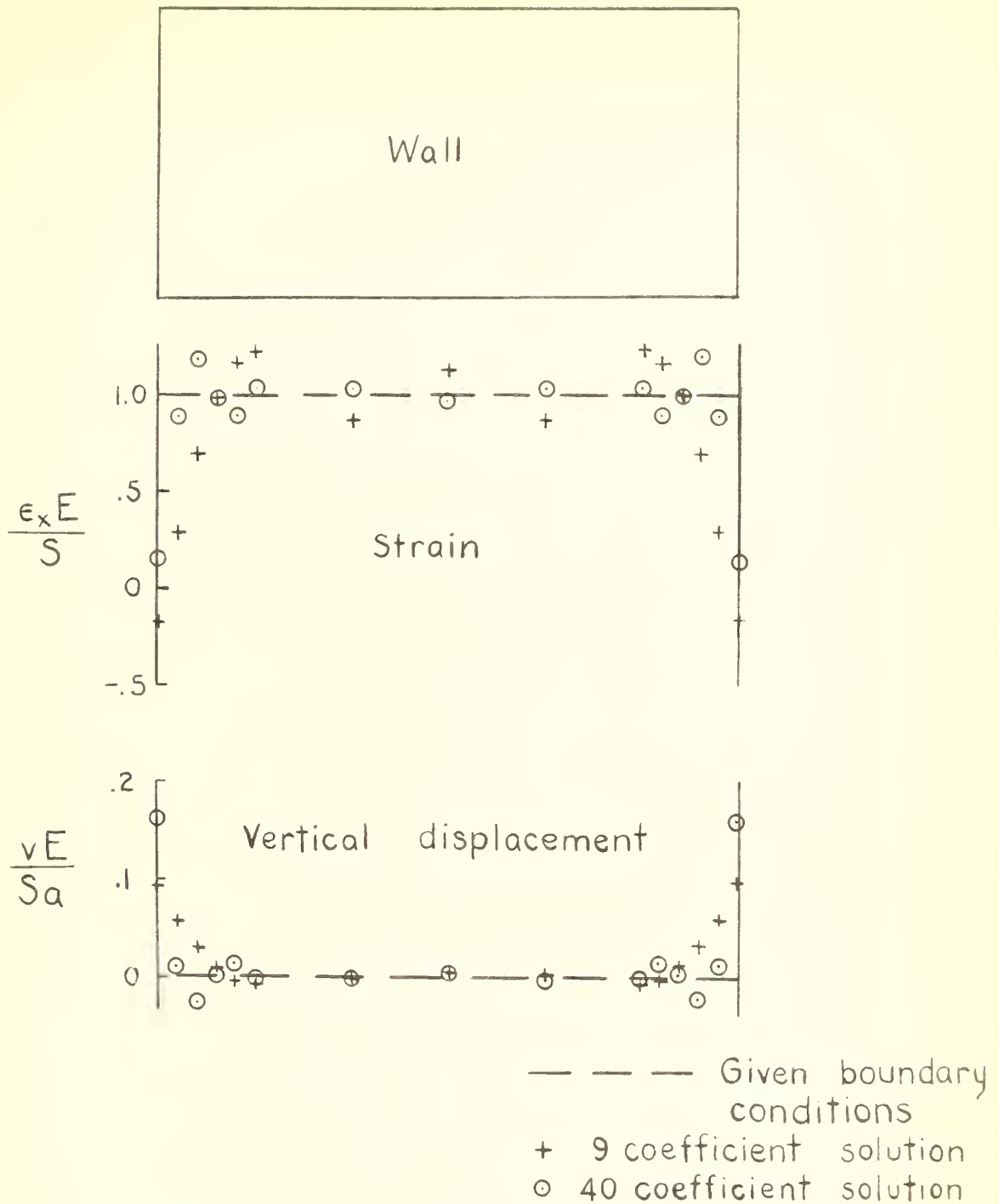
Fig.14 – Agreement of boundary values in solutions
with given boundary conditions along footing.

○ 40 -term solution
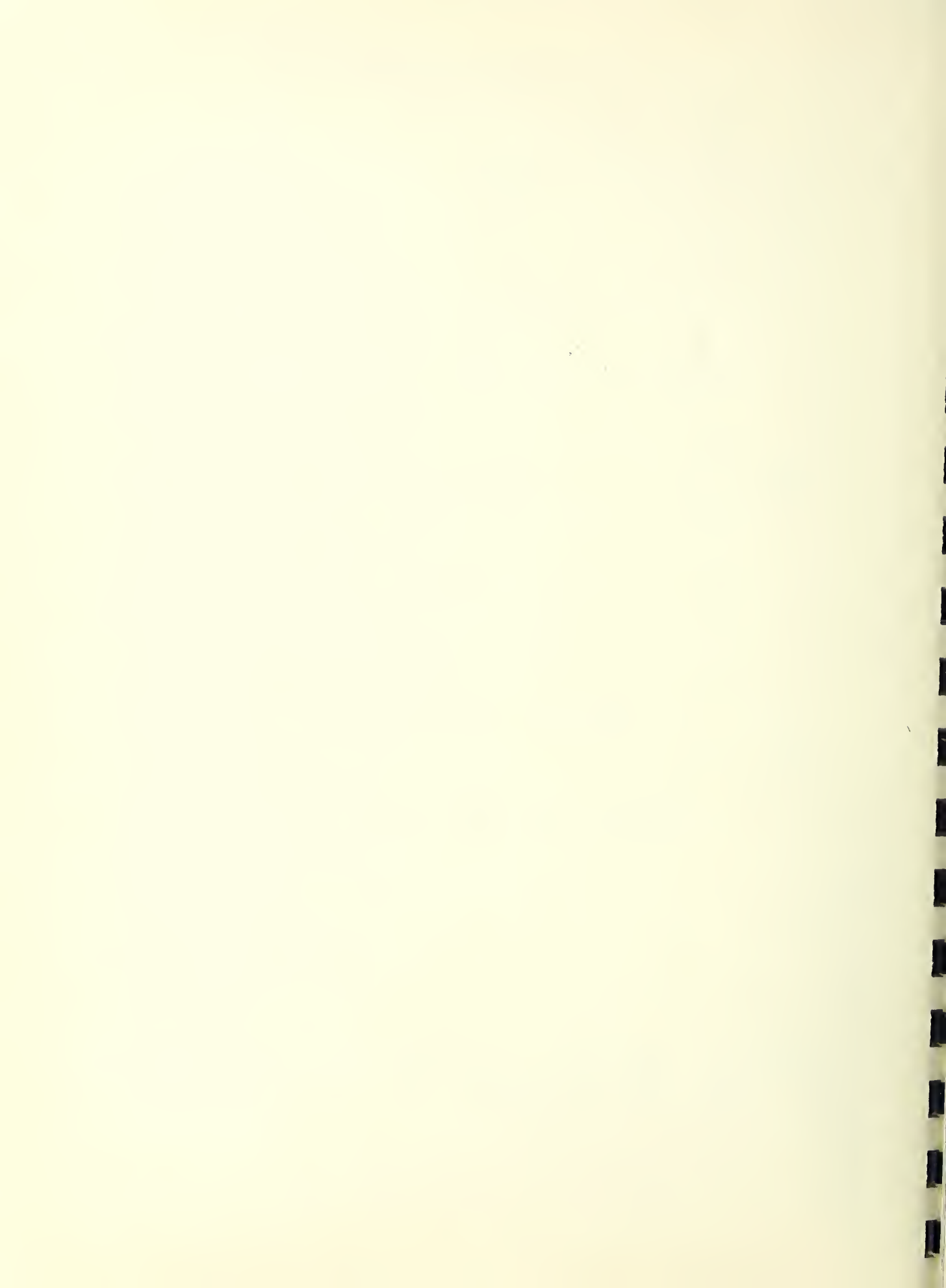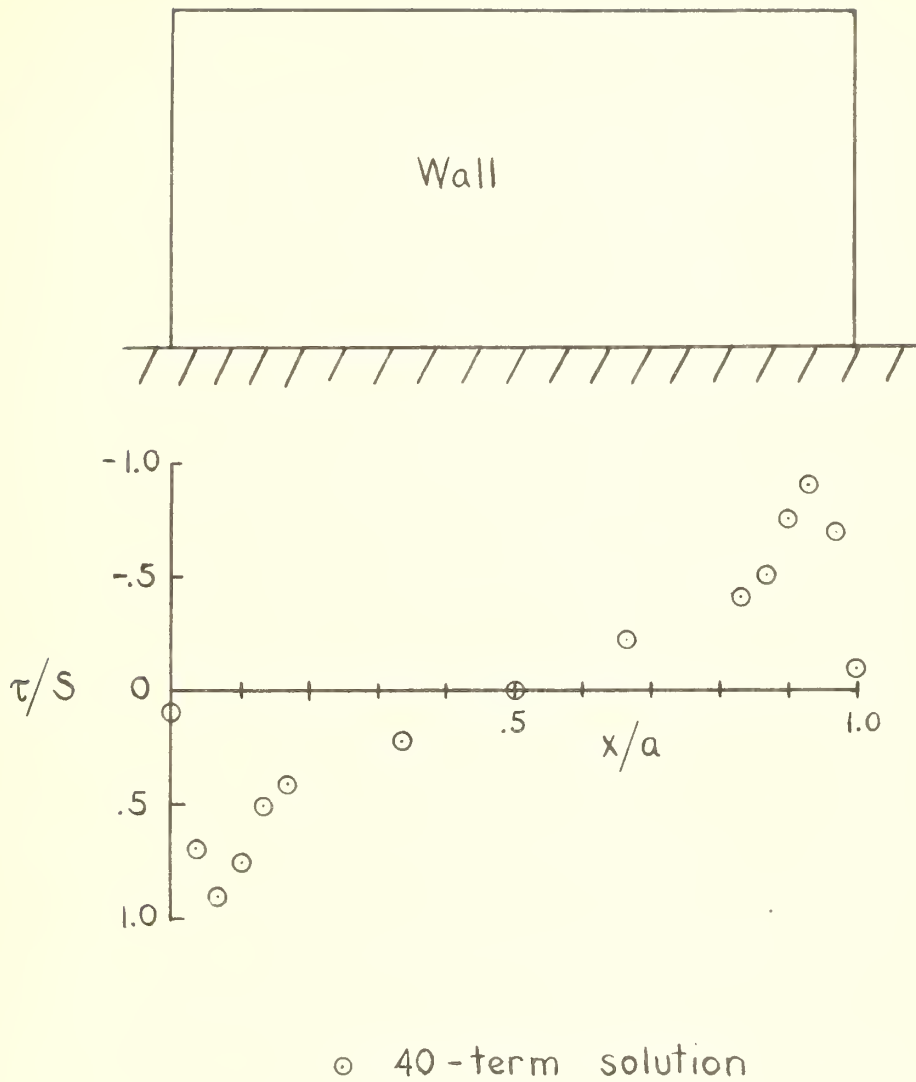
Fig. 15 – Variation of shear stress in wall along base of footing.
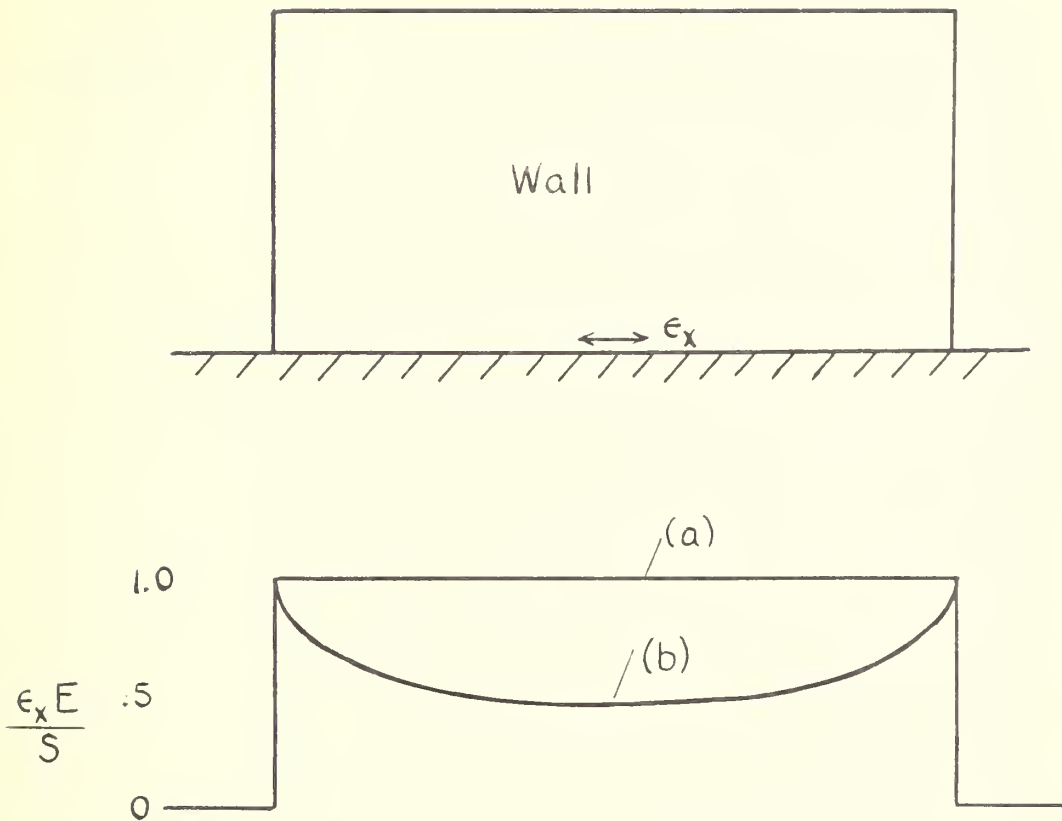
Fig. 16 – Strain distribution along footing -
(a) boundary condition for rigid footing,
section 2.4.1; (b) boundary condition for
test footing, section 2.4.2.

THE NATIONAL BUREAU OF STANDARDS

Functions and Activities

The functions of the National Bureau of Standards are set forth in the Act of Congress, March 3, 1901, as amended by Congress in Public Law 619, 1950. These include the development and maintenance of the national standards of measurement and the provision of means and methods for making measurements consistent with these standards; the determination of physical constants and properties of materials; the development of methods and instruments for testing materials, devices, and structures; advisory services to Government Agencies on scientific and technical problems; invention and development of devices to serve special needs of the Government; and the development of standard practices, codes, and specifications. The work includes basic and applied research, development, engineering, instrumentation, testing, evaluation, calibration services, and various consultation and information services. A major portion of the Bureau's work is performed for other Government Agencies, particularly the Department of Defense and the Atomic Energy Commission. The scope of activities is suggested by the listing of divisions and sections on the inside of the front cover.

Reports and Publications

The results of the Bureau's work take the form of either actual equipment and devices or published papers and reports. Reports are issued to the sponsoring agency of a particular project or program. Published papers appear either in the Bureau's own series of publications or in the journals of professional and scientific societies. The Bureau itself publishes three monthly periodicals, available from the Government Printing Office: The Journal of Research, which presents complete papers reporting technical investigations; the Technical News Bulletin, which presents summary and preliminary reports on work in progress; and Basic Radio Propagation Predictions, which provides data for determining the best frequencies to use for radio communications throughout the world. There are also five series of nonperiodical publications: The Applied Mathematics Series, Circulars, Handbooks, Building Materials and Structures Reports, and Miscellaneous Publications.

Information on the Bureau's publications can be found in NBS Circular 460, Publications of the National Bureau of Standards ($1.25) and its Supplement ($0.75), available from the Superintendent of Documents, Government Printing Office. Inquiries regarding the Bureau's reports and publications should be addressed to the Office of Scientific Publications, National Bureau of Standards, Washington 25, D. C.